Published June 27, 2011

miR669a and miR669q prevent skeletal muscle differentiation in postnatal cardiac progenitors

Stefania Crippa,[1] Marco Cassano,[1] Graziella Messina,[3,4] Daniela Galli,[5] Beatriz G. Galvez,[6] Tomaz Curk,[7] Claudia Altomare,[8] Flavio Ronzoni,[5] Jaan Toelen,[2] Rik Gijsbers,[2] Zeger Debyser,[2] Stefan Janssens,[9] Blaz Zupan,[7] Antonio Zaza,[8] Giulio Cossu,[3,4] and Maurilio Sampaolesi[1,5]

[1]Translational Cardiomyology Laboratory, Interdepartmental Stem Cell Institute, and [2]Molecular Medicine, Catholic University of Leuven, 3000 Leuven, Belgium
[3]Division of Regenerative Medicine, San Raffaele Scientific Institute, 20132 Milan, Italy
[4]Department of Biology, University of Milan, 20129 Milan, Italy
[5]Experimental Medicine Department, Human Anatomy Institute, Center for Tissue Engineering, University of Pavia, 27100 Pavia, Italy
[6]National Center for Cardiovascular Research, 28029 Madrid, Spain
[7]Faculty of Computer and Information Science, University of Ljubljana, 1000 Ljubljana, Slovenia
[8]Department of Biotechnology and Biosciences, Bicocca University, 20126 Milano, Italy
[9]Cardiology Division, University Hospital Gasthuisberg, 3000 Leuven, Belgium

Postnatal heart stem and progenitor cells are a potential therapeutic tool for cardiomyopathies, but little is known about the mechanisms that control cardiac differentiation. Recent work has highlighted an important role for microribonucleic acids (miRNAs) as regulators of cardiac and skeletal myogenesis. In this paper, we isolated cardiac progenitors from neonatal β-sarcoglycan (*Sgcb*)–null mouse hearts affected by dilated cardiomyopathy. Unexpectedly, *Sgcb*-null cardiac progenitors spontaneously differentiated into skeletal muscle fibers both in vitro and when transplanted into regenerating muscles or infarcted hearts. Differentiation potential correlated with the absence of expression of a novel miRNA, miR669q, and with down-regulation of miR669a. Other miRNAs are known to promote myogenesis, but only miR669a and miR669q act upstream of myogenic regulatory factors to prevent myogenesis by directly targeting the MyoD 3′ untranslated region. This finding reveals an added level of complexity in the mechanism of the fate choice of mesoderm progenitors and suggests that using endogenous cardiac stem cells therapeutically will require specially tailored procedures for certain genetic diseases.

Introduction

Stem cell therapy for skeletal and cardiac disease is a promising strategy to promote regeneration of tissues characterized by slow cellular turnover (Nadal-Ginard et al., 2005; Anversa et al., 2006; Yi et al., 2010). Skeletal muscle is actively repaired by satellite cells that sustain tissue regeneration and replace damaged fibers. The heart, in contrast, forms scar tissue after injuries and was once considered a postmitotic organ without regenerative capacity. Data initially obtained from sex-mismatched cardiac transplants led to the identification and characterization of resident stem cells able to migrate into heart ischemic regions (Quaini et al., 2002; Beltrami et al., 2003). Other cardiac stem/progenitor cells with similar characteristics were rapidly identified by several groups on the basis of differential marker expression and ability to differentiate into one or more cell types of the heart (Oh et al., 2003, 2004; Beltrami et al., 2005; Laugwitz et al., 2005). We recently showed that pericyte-derived cells (Dellavalle et al., 2007), termed mesoangioblasts, are present in skeletal muscle and heart, show limited self-renewal, and undergo skeletal (Sampaolesi et al., 2003, 2006) and cardiac (Galvez et al., 2008, 2009) myogenesis, respectively. The number of proliferating cardiac progenitors strongly increases in acute and chronic diseases, although they

Correspondence to Maurilio Sampaolesi: maurilio.sampaolesi@med.kuleuven.be

Abbreviations used in this paper: CMV, cytomegalovirus; cTnI, cardiac troponin I; ctx, cardiotoxin; dpc, day postcoitum; GAPDH, glyceraldehyde 3-phosphate dehydrogenase; H&E, hematoxylin and eosin; HS, horse serum; KO, knockout; LNA, locked nucleic acid; miRNA, microRNA; MyHC, myosin heavy chain; qPCR, quantitative PCR; shRNA, small hairpin RNA; SMA, smooth muscle actin; snRNA, small nuclear RNA; TA, tibialis anterior; UTR, untranslated region; wt, wild type.

Supplemental Material can be found at:
http://jcb.rupress.org/content/suppl/2011/06/24/jcb.201011099.DC1.html

The Rockefeller University Press $30.00
J. Cell Biol. Vol. 193 No. 7 1197–1212
www.jcb.org/cgi/doi/10.1083/jcb.201011099

Published June 27, 2011

Table I. **Characterization of *Sgcb*-null clones by FACS analysis**

Clone	G5 At	G2 At	B5 At	H4 Ven	B9 Ven	B3 Ven	A4 Aor	A9 Aor	D10 Aor
ISL1	+	+	+	−	−	+	−	−	−
Sca1	++	++	++	+++	+++	++	++	+	+
c-Kit	+	+	+	−	+	−	++	+	+

Summary of clones isolated from *Sgcb*-null hearts and characterized for the expression of cardiac stem cell markers (− < 10%; 10% < + < 30%; 30% < ++ < 70%; 70% < +++ < 100%). At, atrium; Ven, ventricle; Aor, aorta.

appear unable to counteract progressive degeneration, likely because they may get exhausted and senescent in repeated and unsuccessful attempts to regenerate the failing heart (Beltrami et al., 2001; Urbanek et al., 2005).

Chronic cardiac diseases are frequent findings in several forms of muscular dystrophy, including limb-girdle muscular dystrophies, caused by mutations in the sarcoglycan proteins that are involved in the maintenance of muscle integrity during contraction. Mutations in the *Sgcb* gene cause LMD2E (limb-girdle muscular dystrophy type 2E), often characterized by severe cardiomyopathy and mild muscle wasting. Similarly, *Sgcb*-null mice develop severe cardiomyopathy with extensive regions of necrosis, fibrosis, and fatty infiltrations (Durbeej et al., 2000). Although not much is known on the control of cardiac differentiation in adult progenitor cells, recent studies have highlighted the role of microRNAs (miRNAs) in controlling different aspects of muscle functions (Bi et al., 2003; Bartel, 2004; van Rooij et al., 2009). miR1 and miR133 modulate muscle growth and differentiation (Liu et al., 2008; van Rooij et al., 2007, 2008), whereas miR206 specifically promotes skeletal myogenesis (McCarthy, 2008; Yuasa et al., 2008; Williams et al., 2009). Moreover, it has been shown that miRNAs governing muscle performance are encoded by myosin genes (van Rooij et al., 2009). So far, all the identified muscle miRNAs indirectly promote myogenesis, rather than acting directly on key regulatory factors for muscle differentiation.

To develop an ex vivo gene therapy approach for LGMD2E, we isolated and characterized cardiac progenitors from *Sgcb*-null mice on the basis of different cardiac progenitor markers (Beltrami et al., 2003; Oh et al., 2003; Laugwitz et al., 2005; Bu et al., 2009). Here, we report that *Sgcb*-null cardiac progenitors display an aberrant activation of skeletal muscle genes that are normally silenced in healthy cardiac progenitors and differentiate into skeletal muscle fibers both in vitro and in vivo. This is because of the lack of miR669q, a novel identified miRNA encoded by the *Sgcb* gene, and the down-regulation of miR669a. miR669q shows high homology with miR669a and the other members of the miR669 family encoded as a cluster in *Sfmbt2* gene, which is involved in epigenetic silencing of skeletal muscle genes (Wu et al., 2007; Liang et al., 2009). To date, among the miRNAs known to regulate skeletal myogenesis, only miR669a and miR669q directly inhibit the MyoD 3′ untranslated region (UTR) and, consequently, skeletal myogenesis. Gain- and loss-of-function experiments show that these miRNAs act within a network to control cardiac–skeletal muscle fate switch in vitro and in vivo. A delay of skeletal muscle regeneration in muscles overexpressing miR669a confirms its important role in myogenic regulation. These data indicate that ex vivo gene therapy for muscle disease might not work in all cases and show that miR669a and the novel miR669q are able to rescue, at least partially, postinfarct cardiac degeneration in *Sgcb*-null mice by inhibiting MyoD expression that otherwise impairs cardiac progenitors.

Results

Sgcb-null cardiac progenitors show an aberrant differentiation pattern toward skeletal muscle

Hearts were collected from 2-wk-old *Sgcb*-null mice, and under a dissecting microscope, the aortic outflow tract, ventricle, or atrium was isolated, further dissected into small fragments, and plated on 1% gelatin-coated dishes as previously described (Tonlorenzi et al., 2007). After an initial outgrowth of fibroblast-like cells, small round and poorly adhering cells appeared. These cells could be detached by gently pipetting and cloned by limiting dilution (Fig. S1 A). We selected three clones for each heart region (atrium: G5, G2, and B5; ventricle: H4, B9, and B3; and aorta: A4, A9, and D10). Southern blot and PCR analyses confirmed the absence of the *Sgcb* gene in selected clones (Fig. S1 B). Cells in culture maintained a relatively constant proliferation rate until 20 population doublings comparable with the wild-type (wt) clone (Fig. S1 C), normal karyotype (Fig. S1 D), and a constant telomerase activity (Fig. S1 E). *Sgcb*-null cardiac clones were analyzed by flow cytometry for the expression of stem cell surface markers. All clones expressed Sca-1, CD34, CD44, and, weakly, CD31 and c-Kit. CD56, CD45, and CD13, markers for skeletal myoblasts, hematopoietic cells, and endothelial cells, respectively, were not expressed (Fig. S1 F and Table I). All clones robustly expressed pericyte markers, such as smooth muscle actin (SMA), NG2, and PDGFR-β (Fig. S1 G) and were positive for AP, whose activity is associated with pericyte cells (Fig. S1 H).

RT-PCR revealed widespread expression of cardiac markers, such as Nkx2.5, Mef2A, GATA4, and Cx43. In contrast, Isl-1, Tbx5, and myocardin were exclusively expressed in atrium, aorta, and ventricle clones, respectively. Atrial natriuretic peptide was expressed only in atrium and ventricle clones (Fig. S1 I). Changes in gene expression were evaluated by time course quantitative PCR (qPCR) on wt (J8 ventricle [Ven] wt) and *Sgcb*-null (H4 Ven knockout [KO]) ventricle clones at 0, 5, and 7 d in serum starvation. Pericyte markers (SMA, PDGFR-β, and NG2) and early cardiac markers (Nkx2.5, Mef2A, and GATA4) were progressively down-regulated during differentiation in both wt and *Sgcb*-null progenitors (Fig. S1 J). As expected,

Published June 27, 2011

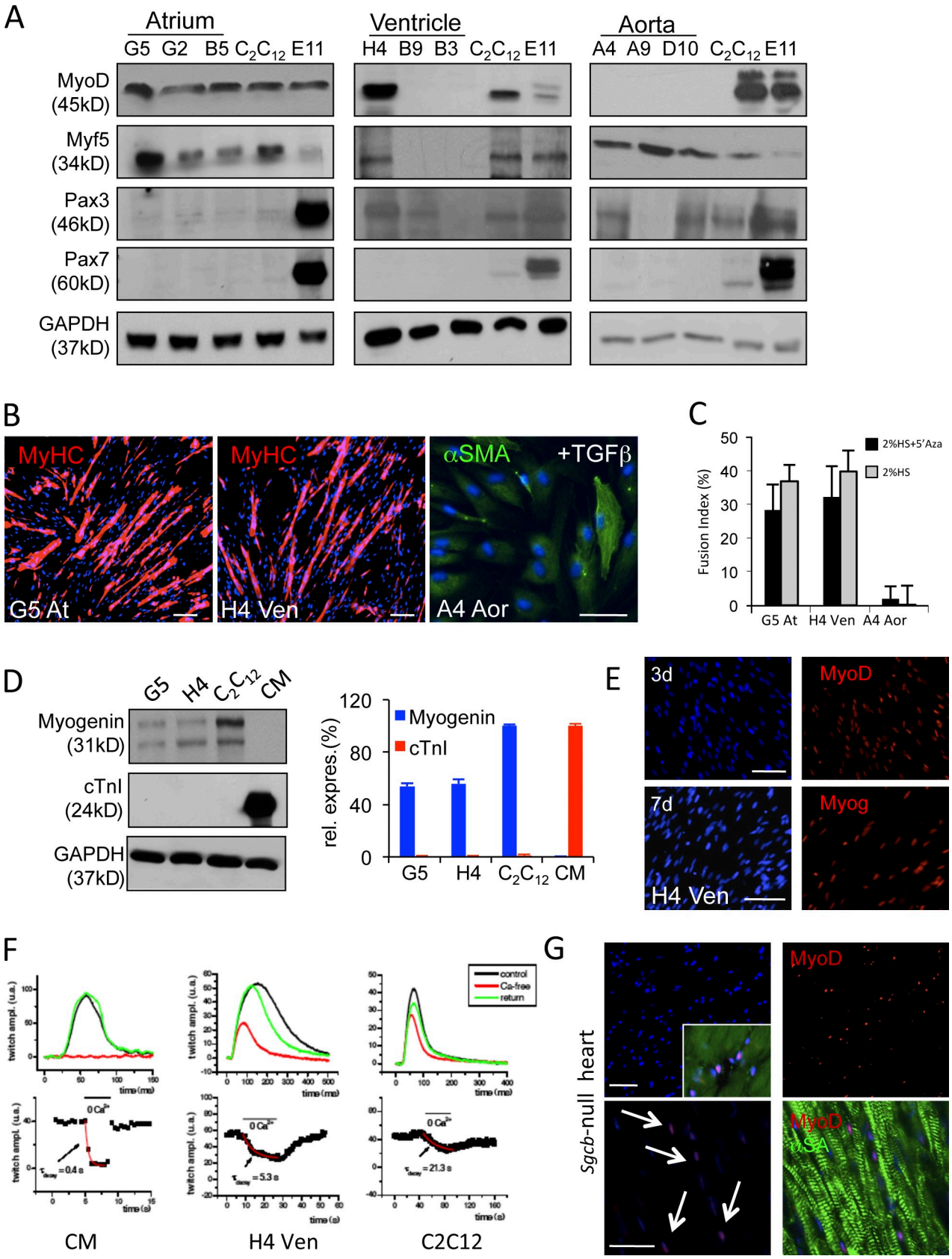

Figure 1. **Myogenic potential of *Sgcb*-null cardiac progenitors.** (A) Western blot analysis for the expression of skeletal muscle transcription factors (MyoD, Myf5, Pax3, and Pax7) in *Sgcb*-null atrium (At; G5, G2, and B5), ventricle (Ven; H4, B9, and B3), and aorta (Aor; A4, A9, and D10) clones. Protein extracts from C2C12 and embryo at 11 d postcoitum (dpc; E11) were used as positive controls. (B) Immunofluorescence analysis of three different *Sgcb*-null clones (G5 atrium, H4 ventricle, and A4 aorta) after 7 d of serum starvation. (C) Fusion index of *Sgcb*-null clones subjected to azacytidine (Aza) treatment

Published June 27, 2011

wt cells progressively up-regulated terminal cardiac differentiation markers (Fig. S2 B; Galvez et al., 2008). Surprisingly, most of the *Sgcb*-null clones up-regulated MyoD and Myf5 skeletal muscle transcription factors but not late cardiac markers as shown by qPCR (Fig. S2 A), Western blot (Fig. 1 A and Fig. S2 B), and microarray analyses (deposited in GEO Datasets under accession no. GSE17774). Despite differences in marker expression, most of the *Sgcb*-null cardiac clones underwent robust skeletal myogenic differentiation after serum starvation as shown by immunofluorescence analysis (Fig. 1 B) and fusion index (Fig. 1 C and Video 1). Differentiation marker analysis indicated that *Sgcb*-null clones expressed approximately half of the myogenin level detected in C2C12 myoblasts but did not express cardiac troponin I (cTnI), normally present in mature cardiomyocytes (Fig. 1 D). Immunofluorescence analysis confirmed MyoD and myogenin expression at early (3 d) and late (7 d) stages of differentiation (Fig. 1 E).

MyoD-negative ventricle clones (B3 and B9) rapidly up-regulated MyoD, Myf5, and myogenin transcription factors during differentiation (Fig. S2, C and D), and they efficiently fused into myotubes (Fig. S2 D). On the contrary, proliferating MyoD-negative aorta clones (A4, A9, and D10) were positive for the expression of early endothelial genes (Fig. S2 E); in the condition of serum starvation, they did not undergo skeletal myogenesis, and upon TGF-β1 treatment, they differentiated into smooth muscle cells (Fig. 1 B, right).

Furthermore, we analyzed the proliferation curves of *Sgcb*-null cardiac clones during 10 d of serum starvation. Cell mortality occurred after 8 d of differentiation because of the pauperization of medium nutrients (Fig. S2 F), when cells have totally fused into skeletal myotubes.

Dependency of contraction on extracellular Ca^{2+} of differentiated *Sgcb*-null cardiac progenitors (H4 Ven KO) was compared with that of C2C12 and neonatal cardiomyocytes. Upon removal of Ca^{2+}, twitch amplitude gradually declined in H4 Ven KO by ∼50%, with a τdecay of 4.6 ± 0.8 s (n = 8). In C2C12, Ca^{2+} decline was observed only in 3 of 10 cells, with a τdecay of 12.3 ± 5.1 s (n = 3). In contrast, Ca^{2+} removal completely suppressed cell twitch in cardiomyocytes (τdecay = 0.8 ± 0.08 s; n = 7; Fig. 1 F). H4 Ven KO showed a contraction pattern compatible with skeletal-type excitation–contraction coupling.

This aberrant myogenic differentiation observed in vitro is recapitulated by the presence of MyoD-positive cells in degenerative foci of 9-mo-old *Sgcb*-null hearts (Fig. 1 G and inset), where, however, terminal differentiation does not occur and multinucleated myofibers are not detected. Considering that MyoD-positive cells were never detected in 2-d-old *Sgcb*-null hearts (Fig. S3 F), we strongly believe that cardiomyocytes of primary and secondary heart fields have additional molecular mechanisms to create a local microenvironment that suppress skeletal muscle differentiation of local cardiac progenitors in the early phase of the disease. Moreover, MyoD-positive nuclei were never revealed in normal hearts or in the hearts of mdx (X chromosome–linked muscular dystrophy) or α-sarcoglycan–null (*Sgca*-null) dystrophic mice (unpublished data) and, thus, are specifically related to the absence of the *Sgcb* gene.

miR669a overexpression rescues cardiac commitment in *Sgcb*-null cardiac progenitors both in vitro and in vivo

We then investigated the mechanism underlying skeletal myogenesis of *Sgcb*-null cardiac clones. Transduction of *Sgcb*-null cardiac progenitors with a lentiviral vector expressing *Sgcb* cDNA (KO + LVbSG) slightly inhibited MyoD expression in *Sgcb*-null cardiac clones (Fig. 2 A), although they maintained the ability to differentiate into skeletal muscle fibers (Fig. 2 B). This excluded a direct role of the SGCB protein in the regulation of cardiac differentiation. However, typical alterations in Ca^{2+} uptake measured in *Sgcb*-null clones were reverted in the presence of the SGCB protein because of restored membrane integrity (Fig. 2 C).

Because the *Sgcb* cDNA and protein were not able to rescue skeletal myogenesis, we evaluated alternative possibilities, such as differentially expressed miRNAs, which were analyzed by miRNA arrays as reported in Fig. S4 (A and B). Among the miRNAs already described to promote skeletal myogenesis, miR206 and miR133b were up-regulated in *Sgcb*-null cardiac clones in comparison with wt counterparts (Fig. S4 A). In addition, we evaluated the expression of muscle-related miRNAs in differentiating *Sgcb*-null cardiac progenitors (Fig. S5 G). miR1 and miR133a involved in controlling differentiation and proliferation of cardiac and skeletal muscle cells (Chen et al., 2005) were up-regulated and down-regulated, respectively. miR27b, a potent inhibitor of Pax3, was down-regulated to ensure rapid and robust entry into the myogenic differentiation program (Crist et al., 2009). The expression of miR221 involved in differentiation and maturation of skeletal muscle cells (Cardinali et al., 2009) didn't change significantly, whereas miR208 expression (van Rooij et al., 2007) was not detected in proliferation or in differentiation conditions (unpublished data).

Interestingly, miR669a, which is highly expressed in wt cardiac progenitors, was almost absent in all *Sgcb*-null clones

(black bars) and serum starvation (gray bars). (D) Western blot analysis for the expression of myogenin and cTnI (left) in the *Sgcb*-null atrium (G5) and ventricle (H4) clones. Extracts from C2C12 and cardiomyocytes (CM) were used as positive and negative controls. Scanner densitometry analysis on three independent experiments for myogenin and cTnI expression is shown on the right. (E) Proliferating (3 d) and differentiating (7 d) *Sgcb*-null ventricle clones were stained with MyoD (top) and myogenin (Myog; bottom). Muscle differentiation assay was performed in triplicates per each sample. (F) Field-stimulated twitches in wt cardiomyocytes, *Sgcb*-null ventricle clone (H4 Ven), and C2C12 cell line. Twitch acquisitions were represented as the arbitrary units (a.u.) during the perfusion of the control Tyrode solution, Ca^{2+}-free, and the return to the control conditions. Time courses of peak amplitudes in the condition of external 0 Ca^{2+} are shown in the bottom graphs. The black bars represent time courses of peak amplitudes in condition of external 0 Ca^{2+}. The red lines represent the monoexponential fitting of time courses yielded time constant values (τdecay). (G) Cardiac sections from 9-mo-old *Sgcb*-null hearts (n = 4) were stained with anti-MyoD (top). Double staining of *Sgcb*-null cardiac sections with MyoD and cardiac MyHC (green) is shown at a lower magnification in the inset (top left). Double staining of *Sgcb*-null cardiac sections with MyoD and α sarcomeric actin (αSA; bottom). Arrows indicate MyoD-positive nuclei in a 9-mo-old *Sgcb*-null heart. rel. expres., relative expression. Error bars show means ± SEM. Bars, 50 µm.

Published June 27, 2011

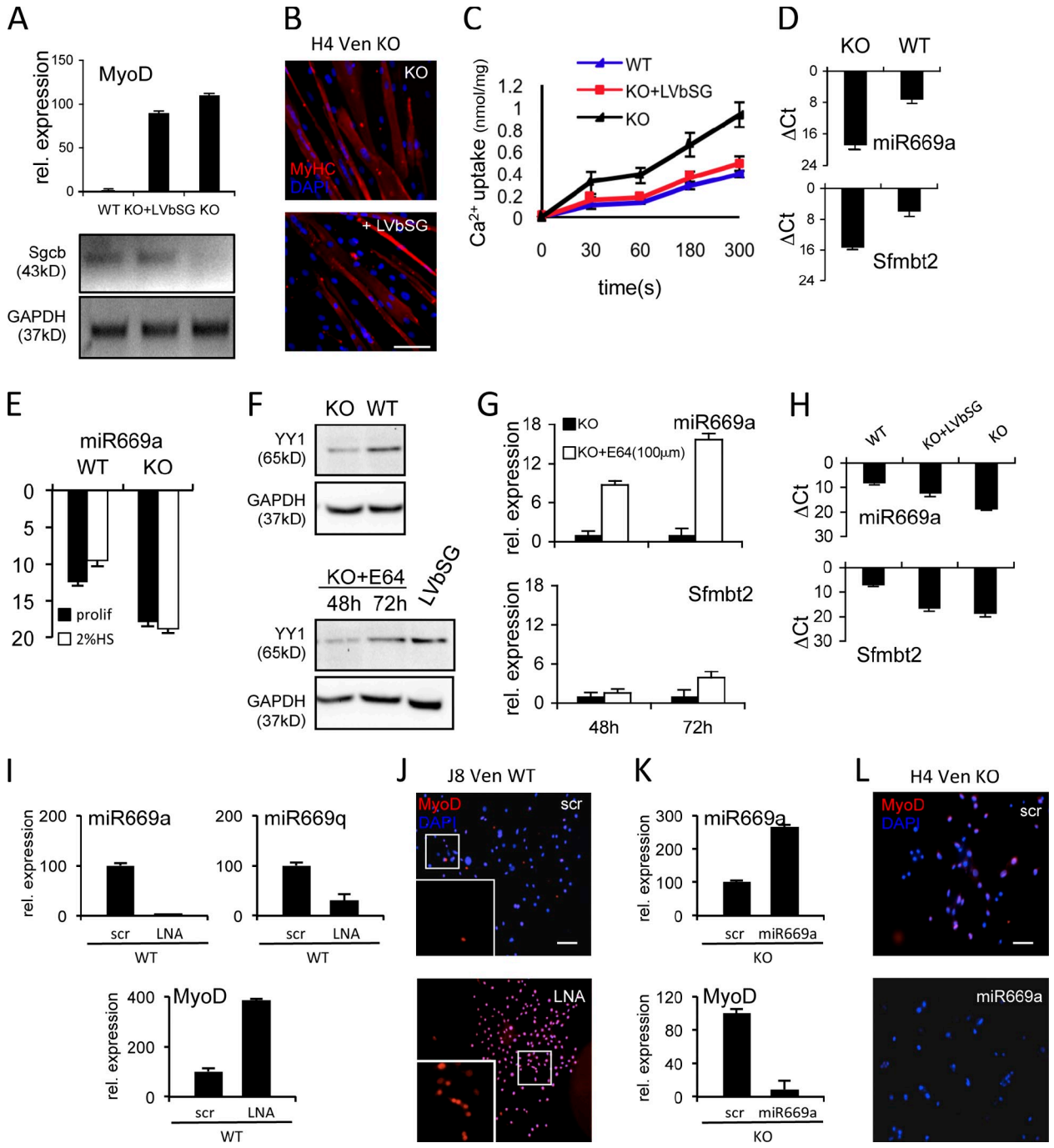

Figure 2. **miR669a overexpression inhibits myogenic differentiation in *Sgcb*-null cardiac progenitors.** (A) qPCR analysis for MyoD expression in wt transduced *Sgcb*-null (KO + LVbSG) and *Sgcb*-null clones (KO; top). Western blot analysis for SGCB expression in differentiating wt, transduced *Sgcb*-null (KO + LVbSG), and *Sgcb*-null clones (KO; bottom). (B) *Sgcb* expression did not interfere with the ability of transduced Sgcb-null cardiac progenitors (+LVbSG) to form myotubes in serum starvation condition similar to not transduced cells (KO). (C) Time course of $^{45}Ca^{2+}$ uptake into wt, transduced *Sgcb*-null (red line), and *Sgcb*-null cells (black line). (D) qPCR analysis for miR669a (top) and *Sfmbt2* (bottom) expression in *Sgcb*-null (KO) and wt clones. Analysis was performed on three independent experiments. (E) miR669a expression in proliferating (prolif) and differentiating (white bars) wt and *Sgcb*-null (KO) cardiac clones.(F) Western blot analysis for YY1 expression in *Sgcb*-null (KO) and wt cardiac progenitors (top), in *Sgcb*-null progenitors treated with E64 for 48 (KO+E64/48h) and 72 (KO+E64/72h) h, and in *Sgcb*-null progenitors transduced with LVbSG (bottom). (G) Relative (rel.) expression of miR669a (top) and *Sfmbt2* (bottom) in *Sgcb*-null cardiac progenitors treated for 48 and 72 h with 100 µM E64 (white bars) and untreated (black bars). (H) miR669a (top) and *Sfmbt2* (bottom) expression analysis in wt and in *Sgcb*-null cardiac progenitors transduced with LVbSG or LV-EGFP (KO). Ct, cycle threshold. (I) TaqMan assay analysis for miR669a and miR669q expression (top) and qPCR analysis for MyoD expression (bottom) in wt cardiac progenitors after transfection with scrambled (scr) miRNA and miR669a LNA knockdown (LNA). miR669a and miR669q silencing activated MyoD expression. (J) MyoD immunofluorescence analysis in the wt cardiac clone (J8 Ven WT) treated with scrambled miRNA (top) and with miR669a LNA (bottom). High magnification of MyoD-positive cells is shown in the insets. (K) miR669a (top) and MyoD (bottom) expression analysis in the *Sgcb*-null cardiac clone (KO) transfected with scrambled miRNA and miR669a. miR669a dramatically reduced MyoD expression in the miR669a-transfected *Sgcb*-null clone. (L) Immunofluorescence analysis for MyoD expression in the *Sgcb*-null cardiac clone transfected with scrambled miRNA (top) and miR669a (bottom). Three independent experiments were performed in triplicates and statistically analyzed using Student's *t* test; $P < 0.05$ in all panels. Error bars show means ± SEM. Bars, 50 µm.

Published June 27, 2011

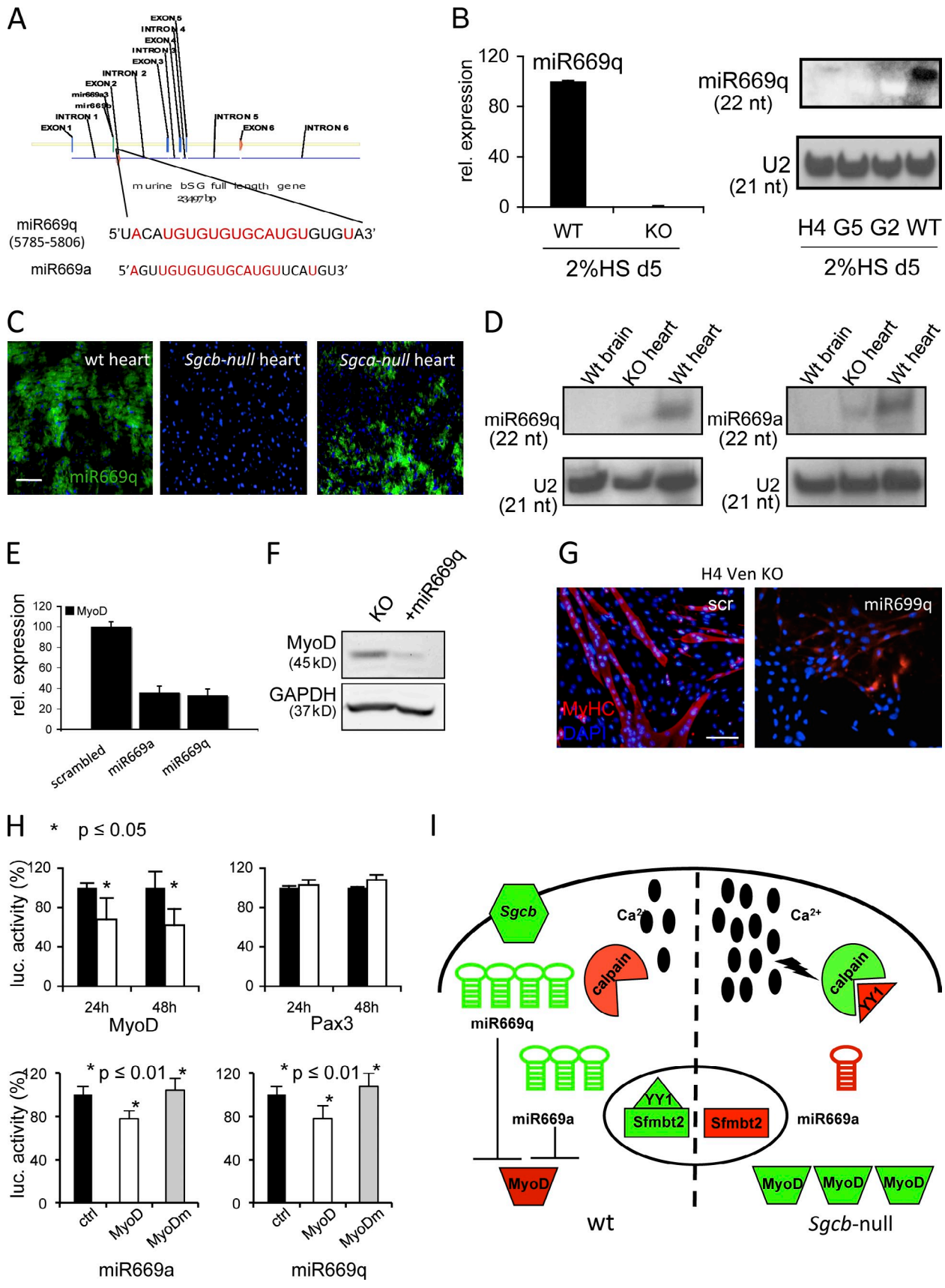

Figure 3. **miR669q and miR669a prevent skeletal myogenesis in postnatal cardiac progenitors.** (A) Schematic representation of miR669q within the *Sgcb* gene. Sequence homology between miR669a and miR669q encoded by the *Sfmbt2* gene (intron 10) and by *Sgcb* (intron 1), respectively, is reported on the bottom. (B) miR669q expression in wt and *Sgcb*-null (KO) clones after 5 d of serum starvation (2% HS d5; left). Northern blot for miR669q expression

Published June 27, 2011

derived from atria and ventricles (Fig. 2, D [top] and E; and Fig. S5 H). Slight differences in the miR669a expression profile are likely associated with different temporal stages toward muscle differentiation of *Sgcb*-null clones.

We also observed that miR669a expression was also reduced in human cardiac progenitors isolated from patients affected by progressive cardiomyopathies (Fig. S5 I), whereas miR206 was up-regulated as shown in Fig. S5 J. Unfortunately, the miR669 family is large and still poorly characterized in humans.

miR669a is encoded by the *Sfmbt2* (*Scm-like with four malignant brain tumor domains 2*) gene, a member of polycomb group proteins involved in epigenetic silencing of skeletal muscle genes (Wu et al., 2007). *Sfmtb2* showed the same expression profile of miR669a, suggesting that the miRNA and the host gene are cotranscribed (Fig. 2 D, bottom). It has been reported that the *Sfmbt2* promoter is positively regulated by the transcription factor *Yy1* (*Yinyang 1*; Kuzmin et al., 2008). Consistent with this finding, we observed that YY1 protein expression was strongly down-regulated in *Sgcb*-null (KO) compared with wt clones (Fig. 2 F, top). YY1 intracellular stability is proteolytically controlled by calpains, a group of nonlysosomal calcium-dependent proteases (Galvagni et al., 1998; Walowitz et al., 1998). The absence of the SGCB protein enhances intracellular calcium level and activates YY1 proteolytic degradation by calpains. We indeed observed that YY1 transcription factor was up-regulated in *Sgcb*-null cardiac clones both when treated with the calpain inhibitor E64 (KO + E64) and after transduction with LVbSG as shown in Fig. 2 F (bottom).

Calpain inhibition (Fig. 2 G) and reduction of Ca^{2+} uptake (Fig. 2 H) partially restored both miR669a and *Sfmtb2* expression in treated *Sgcb*-null clones. Thus, gain- and loss-of-function experiments were performed to possibly correlate miR669a down-regulation in *Sgcb*-null clones with their myogenic commitment. We abolished the expression of miR669a in wt cardiac progenitors (Fig. 2 I, top left) using the locked nucleic acid (LNA) knockdown system. Interestingly, miR669q expression (a so far uncharacterized member of the family; see following paragraph) was also affected by miR669a LNA knockdown (Fig. 2 I, top right). The down-regulation of both miRNAs resulted in the activation of skeletal myogenesis as demonstrated by robust activation of MyoD (Fig. 2 I, bottom) and confirmed by immunofluorescence analysis shown in Fig. 2 J, in which a higher magnification of MyoD-positive nuclei was reported in the inset. Conversely, when *Sgcb*-null cardiac progenitors were transfected with pre-miR669a, MyoD expression was strongly down-regulated (Fig. 2 K, bottom) in miR669a-transfected cells (Fig. 2 K, top). MyoD-positive nuclei were no longer detected after miR669a transfection in *Sgcb*-null cardiac progenitors (Fig. 2 L). Similar results were obtained when *Sgcb*-null cardiac progenitors were transduced with a lentiviral vector carrying both EGFP and two copies of pre-miR669a (Fig. S3 A). Stable expression of miR669a (Fig. S3 B, left) in transduced *Sgcb*-null clones resulted in down-regulation of MyoD (Fig. S3B, right), miR206, and miR133b (not depicted) and up-regulation of cTnI (Fig. S3 B, right). When miR669a-transduced clones were induced to skeletal muscle differentiation, they failed to form myotubes (Fig. S3 C, left; and Video 2) and expressed cTnI (Fig. S3 C, right), indicating that the up-regulation of miR669a switches the differentiation program toward cardiac commitment.

Myogenic commitment was similarly inhibited in *Sgcb*-null cardiac progenitors transfected with MyoD small hairpin RNA (shRNA; Fig. S3 D). Cardiac commitment was partially rescued by MyoD shRNA, although the number of cTnI-positive cells was extremely low (Fig. S3 D, bottom inset). The relation between deletion of the *Sgcb* gene and this miRNA appears to be indirect and hardly specific because most muscular dystrophies result in increased Ca^{2+} entry and enhanced proteolysis. Thus, we examined in detail the structure of the *Sgcb* gene and identified a novel miRNA that we named miR669q, which is encoded in intron 1 of the *Sgcb* gene and homologous to miR669a (Fig. 3 A). miR669q showed a typical hairpin structure (Fig. S4 G) as predicted by mfold (Zuker and Jacobson, 1998).

For the generation of *Sgcb*-null mice, exons 3–6 were replaced by homologous recombination with the neomycin cassette that makes the entire genetic locus unstable. Indeed, *Sgcb* transcripts were never detected in *Sgcb*-null cardiac and skeletal muscle, neither by Northern blotting nor RT-PCR, using a specific probe and primers for exon 2 (which is not deleted by the neomycin cassette; Durbeej et al., 2000).

miR669q was expressed in differentiated wt but not in differentiated *Sgcb*-null cardiac progenitors (KO) as indicated by TaqMan assay (Fig. 3 B, left), Northern blot (Fig. 3 B, right), and in situ hybridization (Fig. 3 C) analyses. miR669q was expressed in the heart of wt and *Sgca*-null mice, a dystrophic animal model with a normal cardiac phenotype. On the contrary, miR669q was absent in *Sgcb*-null hearts, confirming that miR669q expression is abolished by a neomycin cassette inserted in the *Sgcb* gene. The absence of miR669q and miR669a down-regulation in

in differentiated wt and three differentiated *Sgcb*-null clones (H4, G5, and G2) confirmed the absence of miR669q in *Sgcb*-null cardiac progenitors (top right). miR669q signals were normalized for U2 snRNA hybridization. (C) miR669q in situ hybridization on serial sections from adult normal (wt heart) and dystrophic *Sgcb*-null and *Sgca*-null hearts. (D) Northern blot analysis confirmed the absence of miR669q and miR669a down-regulation in *Sgcb*-null hearts. U2 snRNA hybridization was used for sample normalization. (E) MyoD expression analysis in the *Sgcb*-null cardiac clone transfected with scrambled miRNA, miR669a, and miR669q. Three independent experiments were performed in triplicates and statistically analyzed using Student's *t* test. $P < 0.05$. (F) Western blot analysis for MyoD expression in *Sgcb*-null cardiac clone transfected with scrambled miRNA (H4 Ven KO) and miR669q. (G) Immunofluorescence analysis on *Sgcb*-null cardiac clone (H4 Ven KO) transfected with scrambled miRNA (left) and miR669q (right) 7 d after serum starvation (2% HS). (H) Luciferase (luc.) activity was measured in triplicates 24 and 48 h after COS-7 cell transfection with pre-miR669a/MyoD 3′UTR (top left) and pre-miR669a/Pax3 3′UTR (top right). Luciferase activity is indicated by black bars in scrambled transfected cells and by white bars in pre-miR669a/pre-miR669q–transfected cells. Mutagenesis experiments were performed on MyoD 3′UTR target sequence (MyoDm), and luciferase activity was measured in triplicates 24 h after transfection. Luciferase activity was relieved upon mutations of MyoD (gray bars) in both pre-miR669a (bottom left)– and pre-miR669q (bottom right)–transfected cells. Scrambled transfected cells were used as negative controls (ctrl). Error bars indicate standard deviation, and p-values are shown. (I) Schematic representation of the molecular mechanism responsible for the aberrant skeletal muscle differentiation in *Sgcb*-null cardiac progenitors. Active molecules are shown in green; no active molecules are shown in red. Error bars, except for H, show means ± SEM. Bars, 50 µm.

Published June 27, 2011

Table II. **Gene and cell therapy in in vivo experiments**

Treated animals (strain)	Sacrificed animals	Pretreatment	Therapeutic approach	H4 KO cell manipulation	AAV2/9_Lacz virus
8 (Swiss nude)	8	CAL	Sham	–	–
8 (Swiss nude)	8	CAL	Cell	GFP	–
9 (Swiss nude)	6	CAL	Cell	GFP/miR669	–
10 (Swiss nude)	8	TA ctx	Sham	–	–
11 (Swiss nude)	8	TA ctx	Cell	GFP	–
12 (Swiss nude)	6	TA ctx	Cell	GFP/miR669	–
4 (*Sgcb*-null)	4	–	Gene	–	miR669
4 (*Sgcb*-null)	4	–	Gene	–	miRdsRed
12 (Swiss wt)	12	TA ctx	Gene	–	miR669
12 (Swiss wt)	12	TA ctx	Gene	–	miRdsRed
4 (Swiss wt)	3	TA ctx	Oligo	–	miR669q
4 (Swiss wt)	3	TA ctx	Oligo	–	SCR miRNAs

CAL, coronary artery ligation; Oligo, oligonucleotide miRNA precursor from Applied Biosystems; SCR, scramble. Minus signs indicate absence of that specific treatment.

Sgcb-null hearts ($n = 3$) was confirmed by Northern blot analysis (Fig. 3 D).

miR669a and miR669q expression was further analyzed in developing embryos and in adult tissues. miR669q and miR669a were widely expressed in the embryonic heart at embryonic day 13.5 (E13.5; Fig. S5, A and B); conversely, miR669q was not expressed in MyoD-positive somites at E11.5. MyoD and miR669q expression was mutually exclusive (Fig. S5 C, arrowheads). Low levels of miR669q expression colocalized with SMA-positive blood vessels in filter organs (Fig. S5, D–F).

miR669a/miR669q act as a coordinated and synergic system to prevent skeletal myogenesis in cardiac progenitors. Consistently, MyoD expression was strongly inhibited when *Sgcb*-null clones were transfected with miR669a or with miR669q (Fig. 3, E and F). When miR669q-transfected *Sgcb*-null progenitors were induced to differentiate by serum starvation, they failed to fuse into myotubes, although some cells still expressed myosin heavy chain (MyHC), which does not discriminate between cardiac and skeletal myogenesis (Fig. 3 G). Furthermore, MyoD expression was marginally up-regulated in wt cardiac progenitors transfected with antago miR669q, indicating a redundant role of miR669a in MyoD inhibition (unpublished data).

A direct interaction between miR669a and MyoD 3′UTR was confirmed by reduced luciferase activity in COS-7 cells cotransfected with pLuciferase-MyoD 3′UTR, pre-miR669a, and pRL-cytomegalovirus (CMV) vector (used as a transfection efficiency control). No significant reduction of luciferase activity was observed when COS-7 cells were cotransfected with Pax3 3′UTR (Fig. 3 H, top). Similar results were obtained with pre-miR669q–transfected cells (unpublished data).

Consistent with these observations, a target sequence for miR669a and miR669q was identified within the 3′UTR of MyoD (Fig. S4 E). Repression of luciferase activity was partially relieved by mutations affecting MyoD 3′UTR (Fig. S4 F) in pre-miR669a– and pre-miR669q–transfected cells (Fig. 3 H, bottom). The highly conserved central region of miR669a and miR669q mediates MyoD repression even in the absence of perfect seed pairing in both (Shin et al., 2010).

According to our findings, two molecular mechanisms are responsible for the aberrant skeletal muscle differentiation of *Sgcb*-null cardiac clones. The absence of miR669q, not expressed in *Sgcb*-null cardiac progenitors, and the down-regulation of miR669a, caused by the increased intracellular Ca^{2+}, deplete the cell of any negative regulators of MyoD expression (Fig. 3 I).

Next, we investigated the differentiation potential of *Sgcb*-null cardiac progenitors in vivo (Table II). Hearts subjected to ischemic/reperfusion and cardiotoxin (ctx)-injured tibialis anterior (TA) muscles were injected with 5×10^5 H4 KO/GFP and H4 KO/GFP/miR669 transduced *Sgcb*-null clones. Hearts (Fig. 4, A and B) and TA muscles (Fig. 5, A and B) were collected 7 d after injury to localize and evaluate the necrotic area and 5 wk later for immunofluorescence analysis. Transplanted hearts (Fig. 4 C) and TA muscles (Fig. 5 C) were macroscopically similar to sham-operated counterparts. Immunofluorescence analysis for Cx43/GFP on heart sections and laminin/GFP on muscle sections clearly showed that H4 KO/GFP transplanted cells engrafted in both recipient cardiac (Fig. 4 E) and TA muscles (Fig. 5 E). The transplanted H4 KO/GFP/miR669 cardiac clone integrated only in surviving cardiac tissue (Fig. 4 F) and was restricted into the interstitial compartment of injected TA muscles (Fig. 5 F). Quantification of donor cell engraftment is reported in Fig. 5 N. Interestingly, the Cx43 signal was uniformly distributed in sham-operated tissue (Fig. 4 D) together with GFP in H4 KO/GFP/miR669 transplanted hearts (Fig. 4 F, cellular resolution in the inset) but was detected only in GFP negative areas of H4 KO/GFP transplanted hearts (Fig. 4 E). Consistently, serial sections of H4 KO/GFP/miR669 transplanted cardiac tissue showed a large periinfarctual area positive for MyHC and Cx43 as highlighted in Fig. 4 I and with a higher magnification in Fig. 4 I′. Conversely, H4 KO/GFP/miR669 donor cells did not integrate with skeletal muscles fibers when transplanted in TA muscles. Double-positive MyHC/GFP muscle fibers were not detected in H4 KO/GFP/miR669 transplanted mice (Fig. 5, I–I′′) similarly to the sham-operated mice (Fig. 5, G–G′′). On the other hand, H4 KO/GFP transplanted hearts showed several MyHC-positive multinucleated myofibers, which were characterized by the absence of Cx43 (Fig. 4, H [asterisks]

Published June 27, 2011

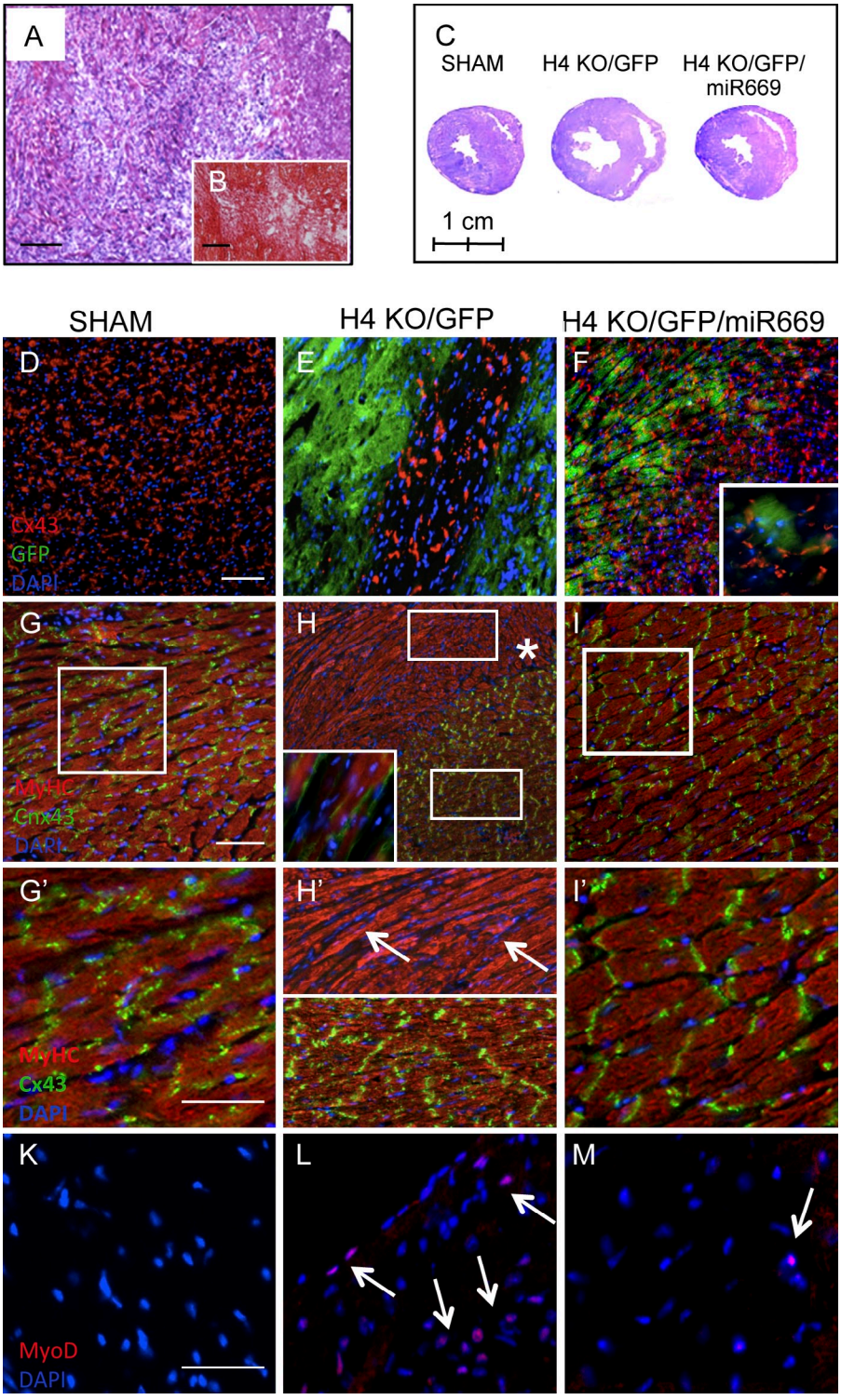

Figure 4. **miR669a overexpression rescues cardiac commitment of *Sgcb*-null cardiac progenitors in vivo.** (A) Hematoxylin and eosin (H&E) staining of heart sections after ischemia/reperfusion. (B) Sirius red specifically stains scare tissue in infarcted hearts. (C) H&E-stained coronal sections of infarcted sham-operated hearts (left) and infarcted hearts transplanted with *Sgcb*-null cells (H4 KO/GFP; middle) or with *Sgcb*-null cells transduced with LVmiR669a (H4 KO/GFP/miR669; right). (D–M) Immunofluorescence analysis on infarcted hearts of sham-operated mice (D, G, G′, and K), infarcted hearts after intraventricular transplantation of 5×10^5 H4 KO/GFP cells (E, H, H′, and L); infarcted hearts after intraventricle transplantation of 5×10^5 H4 KO/GFP/miR669 (F, I, I′, and M). Heart sections of untreated (D) and treated (E and F) mice were stained with anti-Cx43 and anti-GFP. H4 KO/GFP transplanted hearts (E) showed large GFP-positive and Cx43-negative cardiac areas. On the contrary, Cx43-positive cells were homogenously distributed in the sham-operated (D) and in H4 KO/GFP/miR669 transplanted hearts (F). In the inset (F), there is shown a higher magnification of GFP-positive cells expressing Cx43 that are integrated with the surviving cardiomyocytes. Heart sections of untreated (G) and treated (H and I) mice were stained with anti-MyHC and anti-Cx43. High magnification of the highlighted areas in G, H, and I are reported in G′, H′, and I′, respectively. H4 KO/GFP transplanted hearts showed the presence of polynucleated muscle fibers that did not express Cx43, as highlighted by the asterisk in H and arrows in H′. In the inset (H), higher magnification is shown of skeletal MyHC-positive cells in a H4 KO/GFP transplanted heart. On the contrary, sham-operated (G and G′) and H4 KO/GFP/miR669 transplanted hearts (I and I′) showed Cx43 distributed all over the cardiac muscle. Heart sections from untreated (K) and treated (L and M) mice were analyzed for MyoD expression. MyoD-positive nuclei (arrows) are highly expressed in H4 KO/GFP transplanted heart sections (L), whereas they were completely absent in sham-operated heart sections (K) and extremely reduced in H4 KO/GFP/miR669 heart sections (M). Bars: (A, B, and D–I) 50 µm; (G′–M) 100 µm.

and H′ [arrows]), expression of skeletal MyHC (Fig. 4 H, higher resolution shown in the inset) and a large number of MyoD-positive nuclei (Fig. 4 L). MyoD signal was rarely detected in H4 KO/GFP/miR669–treated hearts (Fig. 4 M) and not detected in sham-operated mice (Fig. 4 K). H4 KO/GFP cells participated in muscle regeneration as shown by the colocalization of GFP and MyHC signals (Fig. 5, H–H′′). MyoD-expressing fibers indicated that regeneration was still ongoing in H4 KO/GFP transplanted TA (Fig. 5 L). The number of donor MyoD-positive cells was extremely reduced in H4 KO/GFP/miR669 (Fig. 5 M) and absent in sham transplanted muscle (Fig. 5 K).

To directly investigate the role of miR669a in muscle and cardiac regeneration, we injected AAV2/9-expressing miRdsRed (AAV2/9-nLacZ-miRdsRed2×) as a control or pre-miR669a (AAV2/9-nLacZ-miR669a2×; Fig. 6 A) in *Sgcb*-null cardiomyopathic hearts and in regenerating ctx-injured TA muscles. *Sgcb*-null hearts were analyzed 8 wk after virus injection. The reporter gene was widely expressed in all analyzed sections

Published June 27, 2011

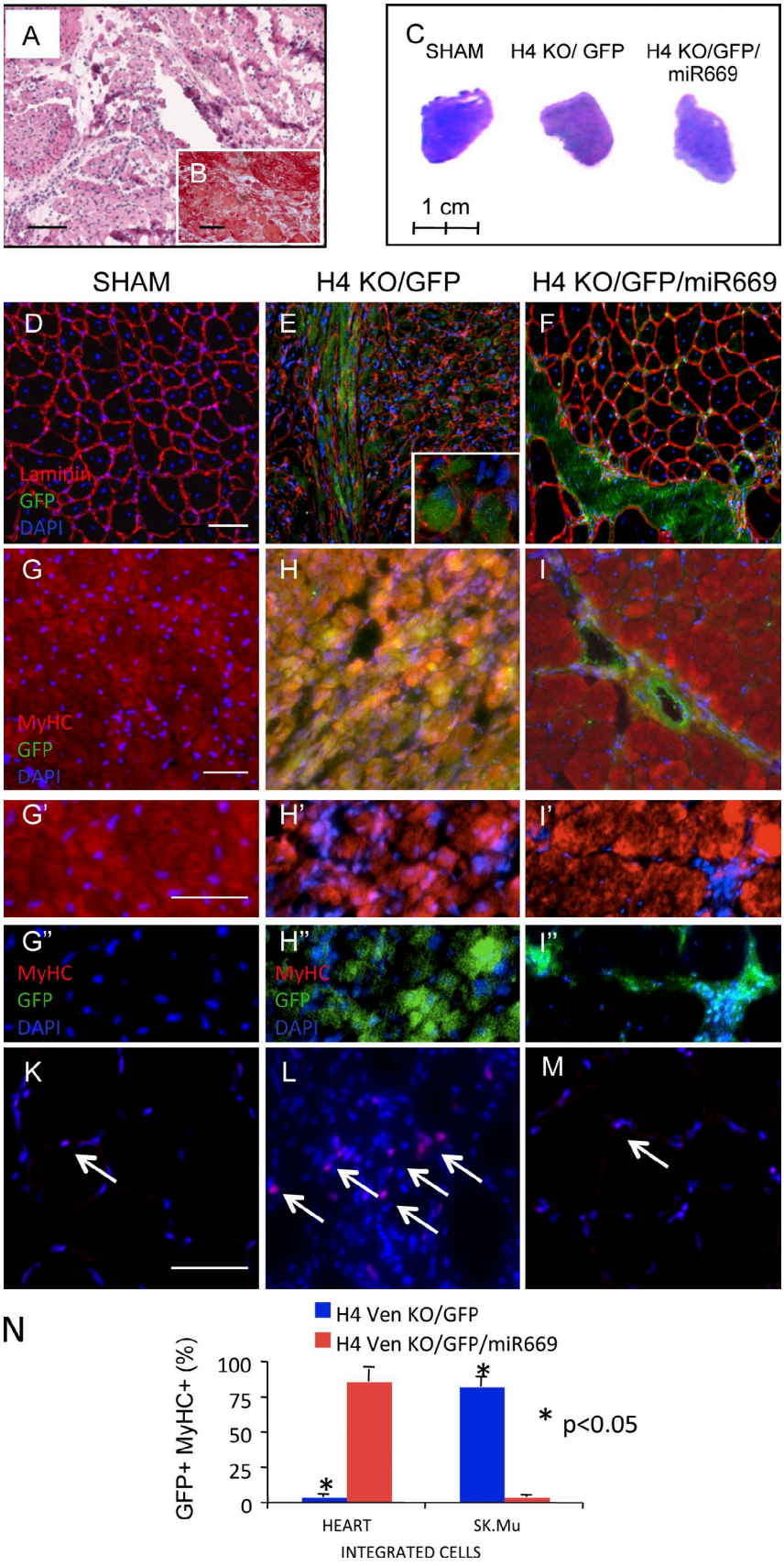

Figure 5. **Myogenic potential of *Sgcb*-null cardiac progenitors is abolished by miR669a overexpression in vivo.** (A) H&E staining of ctx-injured TA muscle sections. (B) Sirius red staining of fibrotic area in muscle sections from ctx-treated TA muscles. (C) H&E-stained coronal sections of ctx-injured muscles sham-operated (left), transplanted with *Sgcb*-null cells (H4 KO/GFP; middle), and with *Sgcb*-null cells transduced with LV-CMV-EGFP-miR669a2× (H4 KO/GFP/miR669; right). (D–M) Immunofluorescence analysis on the ctx-treated sham-operated muscle (D, G–G′′, and K), ctx-treated muscle after a single intramuscular injection of 5 × 10^5 H4 KO/GFP cells (E, H–H′′, and L), and ctx-treated muscle after a single intramuscular injection of 5 × 10^5 H4 KO/GFP/miR669 (F, I–I′′, and M). (D–F) TA muscles were analyzed for the expression of laminin and GFP. GFP-positive cells were specifically localized and integrated with muscle fibers in H4 KO/GFP–injected muscles (E). On the contrary, GFP-positive cells are restricted to interstitial compartment in H4 KO/GFP/miR669-injected muscles (F). As expected, no GFP-positive cells were found in shame-operated muscles (D). Sgcb-null cardiac progenitors transplanted into ctx-damaged TA participate in muscle regeneration. Higher magnification GFP-positive fibers are reported in the inset. (G–I) Muscle sections from untreated (G) and treated (H and I) mice were stained with anti-MyHC and anti-GFP. GFP-positive fibers were differently fused with skeletal muscle fibers in H4 KO/GFP transplanted muscles (H) and shown at a higher magnification in H′ and H′′. MyHC/GFP double-positive fibers were never detected in H4 KO/GFP/miR669 transplanted muscles, in which the only GFP-positive cells were localized in the interstitial and vessel compartment as shown in I–I′′. MyHC/GFP double-positive fibers or GFP-positive cells were not found in the sham-operated muscles (G–G′′). (K–M) MyoD expression was analyzed in untreated (K) and treated (L and M) TA muscles. MyoD was strongly expressed in H4 KO/GFP transplanted muscle fibers (L) and extremely reduced in untreated (K) and in H4 KO/GFP/miR669 (M) transplanted muscle fibers. Arrows indicate MyoD-positive nuclei. (N) Cell counts of GFP/MyHC double-positive cells were performed on muscle and cardiac sections from transplanted mice. Six mice per each group of treatment were independently and statistically analyzed using Student's *t* test ($P < 0.05$). Sk.Mu, skeletal muscle; Ven, ventricle. Error bars show means ± SEM. Bars: (A, B, and D–I) 50 µm; (G′–M) 100 µm.

Published June 27, 2011

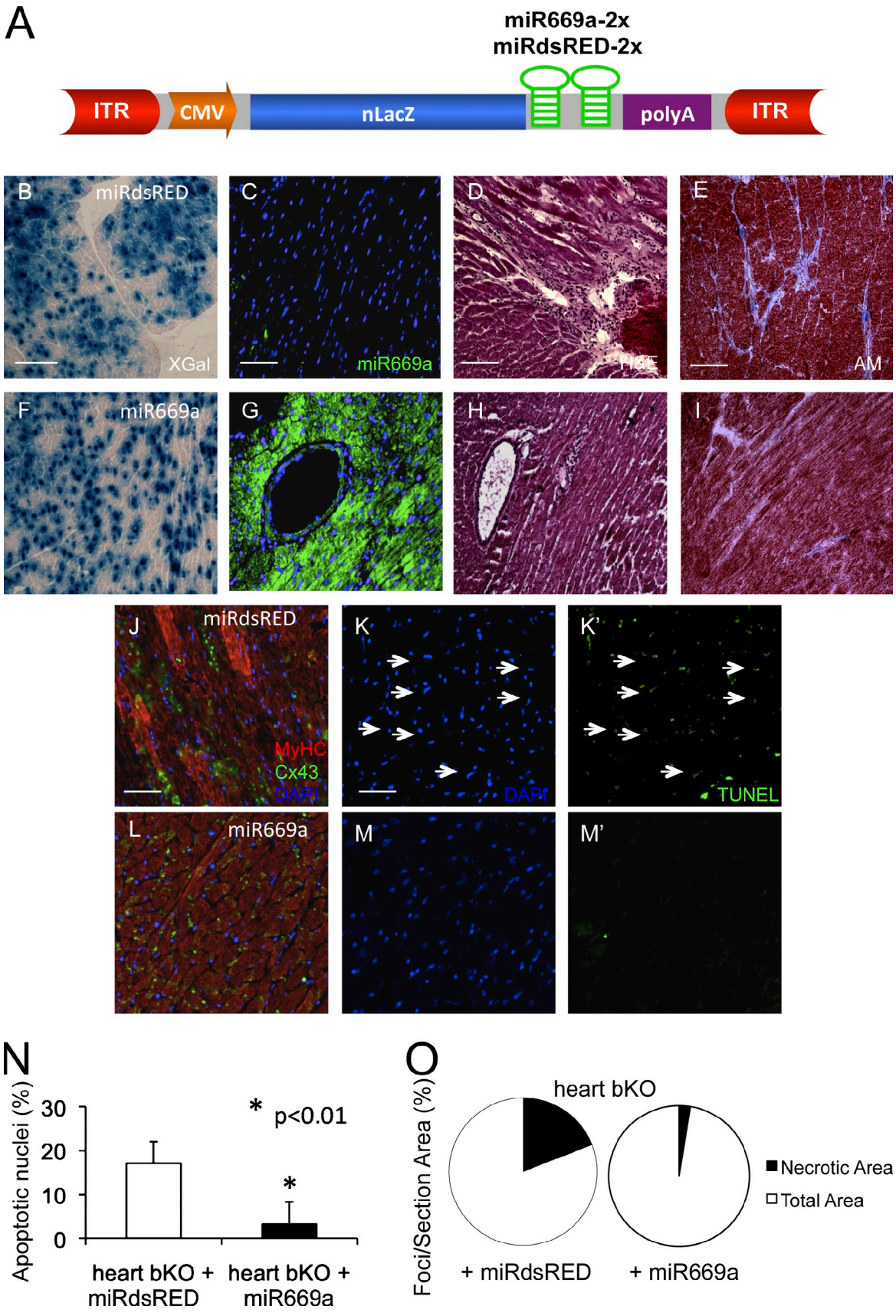

Figure 6. **Overexpression of miR669a ameliorates the dystrophic cardiac phenotype in *Sgcb*-null hearts.** (A) Schematic representation of AAV2/9-TF-CBA-nLacZ-mi669a2×/miRdsRed2×. 2-d-old *Sgcb*-null mice were injected intraventricularly and analyzed 8 wk later (B–L). X-gal reaction, miR669a in situ hybridization, and H&E and Azan-Mallory (AM) staining on heart sections from miRdsRed (B–E)- and miR669a (F–I)-injected animals. miR669a was

Published June 27, 2011

(Fig. 6, B and F), whereas miR669a was specifically expressed in miR669a-injected hearts (Fig. 6, C and G). We observed amelioration in tissue histology and a delay in the onset of cardiac degeneration (Fig. 6, compare D and E with H and I). Necrotic foci normalized for section area were quantified and reported in Fig. 6 O, showing a reduction of necrosis in miR669a-overexpressing *Sgcb*-null hearts. Immunofluorescence analysis for Cx43 and MyHC also confirmed improved sarcomeric organization (Fig. 6, compare J with L). Furthermore, the number of apoptotic nuclei was dramatically reduced as shown by TUNEL assay (Fig. 6, compare K and K′ with M and M′) and quantified as the percentage of total nuclei per section (Fig. 6 N).

Conversely, in skeletal muscle regeneration, we observed a negative effect of miR669a overexpression that resulted in less efficient muscle regeneration (Fig. 7, A–I). 21 d after viral injection, treated muscles showed a wide expression of the reporter gene (Fig. 7, A and D). Smaller (Fig. 7, compare B and E) and central nucleated fibers positive for β-galactosidase (Fig. 7, compare C and C′ with F and F′) were observed in miR669a-injected muscles, revealing a delay of muscle regeneration specifically induced by miR669a and quantified by morphometric analysis in Fig. 7 I. miR669a-mediated down-regulation of MyoD results in MyHC reduction (Fig. 7 G) as quantified by scanner densitometry in Fig. 7 H. Similar results were obtained for ctx-injured TA after miR669q injection ($n = 3$). Analyzed muscle sections showed higher numbers of centronucleated fibers (Fig. S3 E, arrows), which were smaller in diameter and positive for embryonic MyHC (Fig. S3 E, arrowheads) compared with scramble-treated muscles. Collectively, these results show that overexpression of miR669a is able to rescue, at least partially, cardiac degeneration in *Sgcb*-null mice by inhibiting MyoD expression that otherwise impairs cardiac progenitors. A delay of skeletal muscle regeneration confirms the important role of those specific miRNAs in myogenesis regulation.

Discussion

Together, our data unequivocally show that cardiac progenitors isolated from a mouse model of muscular dystrophy with cardiac involvement (LGMD2E) undergo aberrant differentiation toward skeletal muscle both in vitro and in vivo, independent of the site of transplantation (i.e., cardiac or skeletal muscle). Lineage promiscuity between skeletal and cardiac myogenic progenitors is extremely rare and has been reported only in a single study in which progenitor cells from adult murine skeletal muscle could be induced to differentiate into beating cardiomyocytes (Winitsky et al., 2005).

Cardiac progenitors from *Sgcb*-null hearts undergo this aberrant differentiation because they lack two key regulatory microRNAs, miR669a and miR669q, which are capable of suppressing skeletal myogenesis (Fig. 3, Fig. 4, and Fig. 5). miR669a is encoded and cotranscribed with the host gene *Sfmbt2*, which we found down-regulated in *Sgcb*-null cardiac progenitors because of a signal cascade involving intracellular calcium, calpain proteases, and degradation of YY1, a positive regulator for *Sfmbt2*.

The high level of intracellular Ca^{2+} activates calpain proteases responsible for YY1 proteolytic degradation (Galvagni et al., 1998; Walowitz et al., 1998) in most dystrophic muscle cells (Sampaolesi et al., 2001). On the contrary, miR669q expression is abolished exclusively in *Sgcb*-null cardiac progenitors, depleting the cell of any negative regulator of MyoD expression.

Dysregulation of both miRNAs is necessary to activate skeletal myogenesis in *Sgcb*-null cardiac progenitors. Of notice, miR669a and miR669q are the first identified miRNAs that act upstream of MyoD, thus indirectly regulating all MyoD targets.

When cardiac progenitors from dystrophic mice were transplanted into female nude mice after focal damage caused by ctx treatment in skeletal muscle and coronary ligation in the heart, they readily engrafted into cardiac and skeletal muscles. Donor-derived *Sgcb*-null cells were unable to restore cardiac tissue and persistently differentiated in skeletal muscle that altered the regular heart beating (Video 3). Skeletal myoblasts have been shown to do so in an infarcted human heart even though they elicit a functional benefit (Menasché et al., 2008). The inability of *Sgcb*-null cardiac progenitors to differentiate into cardiomyocytes after transplantation into an injured heart demonstrates that their normal differentiation potential has been subverted and a regenerating cardiac environment is not sufficient to rescue it. It thus becomes important to ask why skeletal muscle does not form aberrantly in the heart of *Sgcb*-null mice. Probably, cardiomyocytes of primary and secondary heart fields have additional molecular mechanisms to suppress skeletal myogenesis and, thus, create a local microenvironment that suppresses the skeletal muscle differentiation of local cardiac progenitors. This theory is consistent with a large number of apoptotic cells in regeneration/degeneration foci of the dystrophic heart, in which MyoD-expressing cells are detected during the progression of the disease. This may explain, at least in part, the failure of cardiac progenitors to efficiently counteract cardiac degeneration in *Sgcb*-null mice and may relate to aberrant MyoD expression in oncocytic (Hotárková et al., 2004) and Myf5-induced cardiomyopathy (Santerre et al., 1993).

So far, no function was associated with the miR669 family. Here, we show that both miR669a and the novel miR669q are critical to prevent skeletal muscle differentiation in cardiac tissue. This would suggest that skeletal myogenesis is dominant

specifically expressed in miR669a-injected *Sgcb*-null hearts (C and G). Necrotic foci and fibrotic area extension were reduced in miR669a (H and I) compared with miRdsRed (D and E)-treated *Sgcb*-null hearts, assuming a benefic role of miR669a overexpression in cardiac pathology progression. Immunofluorescence analysis for MyHC and Cx43 expression in miRdsRed (J)- and miR669a (L)-injected *Sgcb*-null hearts. TUNEL assay analysis on miRdsRed (K and K′)- and miR669a (M and M′)-injected *Sgcb*-null hearts. Apoptotic nuclei are shown in green and highlighted by arrows in K and K′. (N) Percentage of apoptotic nuclei on cardiac sections from miRdsRed- and miR669a-injected *Sgcb*-null hearts. Three mice per each group of treatment were independently and statistically analyzed using Student's *t* test ($P < 0.01$). (O) Percentage of necrotic foci on total cardiac section of miRdsRed- and miR669a-injected *Sgcb*-null hearts. Four mice per each group of treatment were independently and statistically analyzed. Bars, 50 µm.

Published June 27, 2011

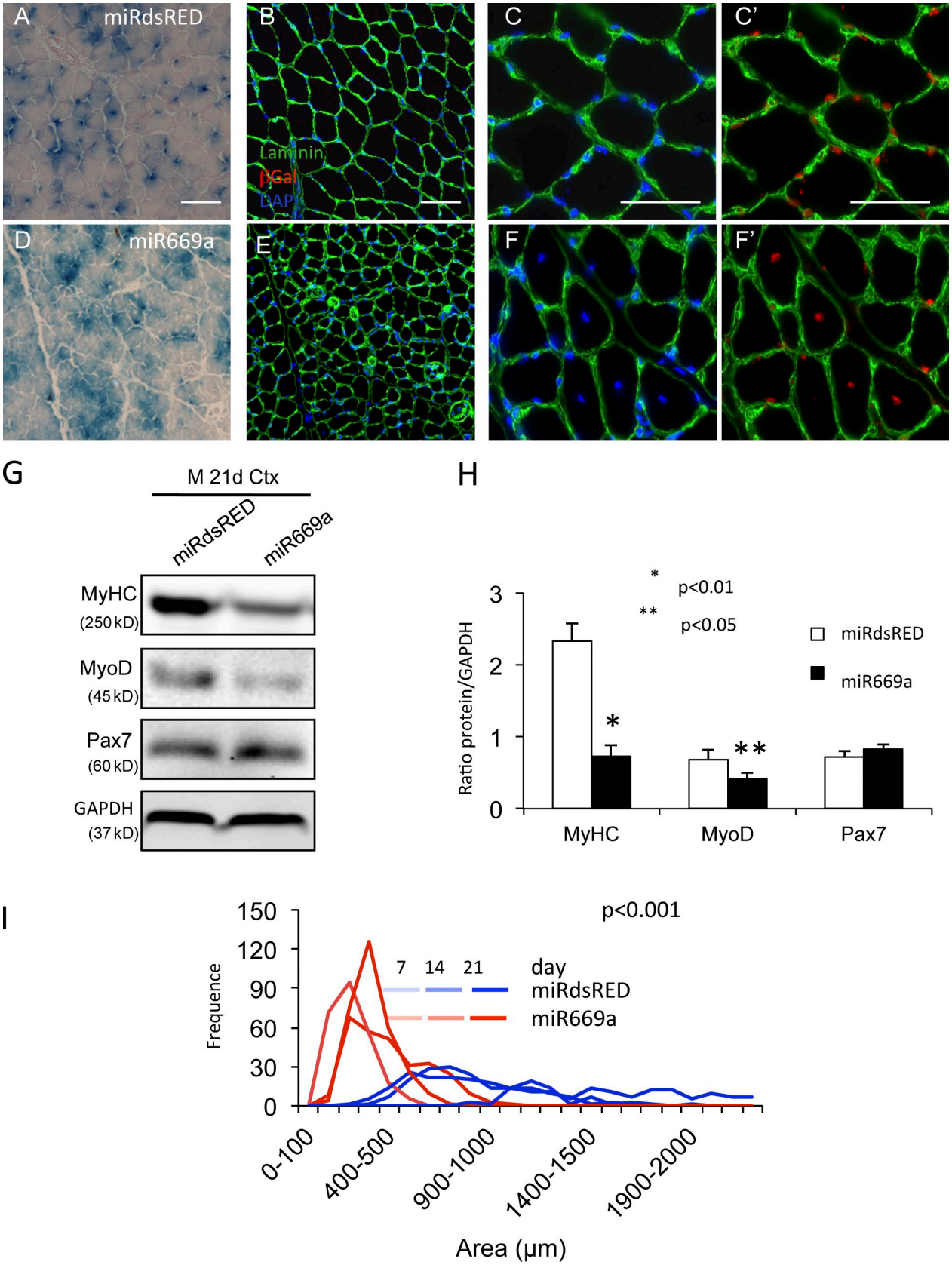

Figure 7. **Overexpression of miR669a delays skeletal muscle regeneration in ctx-injured TA muscles.** TA muscles of 7-d-old Swiss mice were ctx injured, injected intramuscularly with AAV2/9-nLacZ-miR669a2× (miR669a), and analyzed 7, 14, and 21 d after injury. AAV2/9-nLacZ-miRdsRed2× (miRdsRED) was used as a negative control. (A, B, D, and E) X-gal reaction on miRdsRed (A) and miR669a (D) treated muscle sections. Laminin expression in miRdsRed (B)- and miR669a (E)-treated muscle sections. miR669a-treated muscles showed smaller fibers compared with control muscles. (C, C′, F, and F′) Laminin

Published June 27, 2011

(possibly because of the dominant nature of MyoD) and requires active suppression in closely related mesoderm lineages that express many common regulatory factors. These experiments lead to the conclusion that miR669a and miR669q regulate the cell fate of cardiac progenitors by directly targeting MyoD expression through their central region.

Redundancy of the miR669a/miR669q system and two different regulation mechanisms guarantee a tight inhibition of the skeletal myogenic program in cardiac progenitors, in which it is not required. Calpain activation in *Sgcb*-null cardiac progenitors reduced the expression of miR669a and all the members of the 669 cluster that are encoded in the *Sfmbt2* gene and share homology with miR669a in the central region. Conversely, miR669q is cotranscribed with the *Sgcb* gene in muscle cells and not regulated by calpains. However, the role of miR669a and miR669q in skeletal muscle homeostasis and physiological relevance is currently under investigation.

In conclusion, at least two members of miR669 family, miR669a and miR669q, are capable of repressing skeletal myogenesis in wt cardiac progenitors by directly inhibiting MyoD expression, revealing a mechanism that had not been described or predicted until now. Although these data indicate that the simple scheme isolation–genetic correction–autologous transplantation may not work in all cases, it also raises intriguing questions about human LGMD2E that remain to be addressed but depend upon the extremely problematic availability of cardiac biopsies from these patients and the fact that the miR669 family has not yet been characterized in human hearts.

Materials and methods

Isolation and skeletal muscle differentiation of *Sgcb*-null cardiac progenitors

Sgcb-null mice were generated by the group of K.P. Campbell (University of Iowa, Iowa City, IA). Hearts isolated from 2-wk *Sgcb*-null mice were kept in DME without FCS with antibiotics and divided in three different pieces: aorta, ventricle, and atrium. Each piece was rinsed in PBS with Ca^+/Mg^+ and sharply dissected into 1–2-mm-diameter pieces with a scalpel. Fragments containing small vessels were transferred to a Petri dish coated with 1% gelatin in the presence of 20% FBS-DME plus 5 mM glutamine and antibiotics. These heart fragments were cultured for 8–15 d depending on the region, and after the initial outgrowth of fibroblast-like cells, small round and refractile cells appeared. This cell population was easily collected by gently pipetting of the original culture, counted, and cloned by limited dilution on 1% gelatin-coated p96 well dishes. Different valid clones were selected by phase-contrast morphology. In some experiments, cells were prospectively isolated from collagenase-digested neonatal hearts by the expression of c-Kit following a previously published protocol (Beltrami et al., 2001). The cells obtained showed a similar phenotype to those isolated by the explant methods.

Skeletal muscle differentiation was induced by 5′azacitydine and, spontaneously, in differentiation medium (DME 2% horse serum [HS]). After 7 d, cultures were fixed and stained with antibodies against MyHC and MyoD. Western blot analysis was performed using the same antibodies.

Inhibition and activation of myogenic differentiation

Skeletal muscle differentiation was inhibited in *Sgcb*-null and activated in wt cardiac progenitors by transfection with pre-miR669a (Invitrogen) and miR669a LNA knockdown transfection (Exigon), respectively, according to the Lipofectamine 2000 manufacturer's instructions (Invitrogen).

Lentiviral vector production and *Sgcb*-null cardiac progenitor transduction

Lentiviral vector encoding *Sgcb* (LV-CHMWS-*Sgcb*-IRES-GFP) was generated by PCR amplification of differentiated C2C12 cDNA using the following primers: *Sgcb* forward, 5′-AAAAAAAGATCTATGGCGGCAGCGGCGGCGGGCG-3′, and reverse, 5′-AAAAAATCTAGACTAATGAGTGTTCCCACAAGGGTTGTC-3′. The unique restriction sites XbaI and BglII were added to the 5′ and 3′ ends of *Sgcb* forward and *Sgcb* reverse primers, respectively. After amplification, the *Sgcb* PCR product was digested with XbaI and BglII and cloned into the pCHMWS-IRES-GFP digested with BamHI and NheI, which generate compatible ends for XbaI and BglII, respectively.

Lentiviral vector encoding two copies of pre-miRNA669a was generated by PCR amplification of the pre-miRNA669a template using the following primers: miR669a forward, 5′-AAAAAAGATCTCGAGATTCCTCCATGTATGTGCATGTGTGTATAGTTGTG-3′, and reverse, 5′-AAAAAAGGATCCAAGTCGACTGTGTCTGTGTATGTGTGCTTGCGTTTATACGTGTG-3′. The unique restriction sites BglII–XhoI and BamHI–SalI were added to the 5′ and 3′ ends of miR669a forward and miR669a reverse primers, respectively. After amplification, the pre-miR669a PCR product was digested with XhoI and BamHI and inserted two times into the transfer plasmid pN3-MCS-WPRE-EGFP C12. The 2× pre-miR669a fragment was excised using XhoI and KpnI and cloned into pCHMWS-EGFP digested with the same restriction enzymes, resulting in LV-CHMWS-EGFP–pre-miRNA669a2×. Third generation lentiviral particles were generated by transient transfection in 293T cells and were used to infect *Sgcb*-null clones at MOI 50. GFP was used as a standard gene expression tracer for in vivo experiments.

Adeno-associated vector production and injection into injured muscles and cardiomyopathic hearts

An adaptor containing ApaI and AsuII restriction sites was generated by the annealing of the following primers: adaptor adeno-associated viral vector forward, 5′-TCGAAGCTTACCGGTACTAGTGGGCCCAATTGTTCGAAGC-3′, and reverse, 5′-GGCCGCTTCGAACAATTGGGCCCACTAGTACCGGTAAGCT-3′, and ligated into SalI–NotI-digested pN3-WPRE-EGFP-miR669a2× C12 transfer plasmid. The miR669a2× cassette was excised using NheI and ApaI and cloned into pAAV-EnhCB-LacZnls digested with the same restriction enzymes. AAV2/9-lacZnls-miR669a2× viral particles were used to inject TA muscle 5 d after ctx injury (10^9 transduction units) and to inject intraventricular *Sgcb*-null hearts affected by cardiomyopathy (10^9 transduction units). AAV2/9-lacZnls-miRdsRed2× was produced with the same protocol and used as a negative control.

Northern blot analysis

The miRNA population was isolated from proliferating and differentiated wt and *Sgcb*-null cardiac clones and hearts according to an miRNA isolation kit (PureLink; Invitrogen). 1 µg miRNA sample was heated at 95°C for 5 min and run on denaturating acrylamide gel (15 ml of gel; 1.5 ml of 10× TBE (Tris/borate/EDTA)/8 M urea, 5.6 ml acrylamide/bisacrylamide [19:1], 75 µl ammonium persolphate, 15 µl tetramethylethylenediamine, and H_2O to final volume) at 100 V until bromophenol blue reached the bottom of the gel (~90 min). After ethidium bromide staining of polyacrylamide gels, the tRNA and 5 and 5.8 S RNA bands were visualized under a UV transilluminator and served as loading controls. Then miRNAs were transferred to a nylon membrane (Hybond-N+; GE Healthcare) by electroblotting for 2 h at 200 mM. RNA was then UV cross-linked to the nylon membrane (120-mJ burst for 1 min.). miR669a and miR669q were detected on a Northern blot using specific [P^{32}]ATP-labeled probes. After 2 h at 37°C in prehybridization solution (6× SSC, 10× Denhardt's solution, and 0.2% SDS), the membrane was incubated for 24 h in the hybridization

and β-galactosidase expression on miRdsRed (C and C′)- and miR669a (F and F′)-injected muscle sections. Muscle fibers with central position of β-galactosidase–positive nuclei were predominantly found in miR669a-treated muscles (F′). (G) MyHC, MyoD, and Pax7 expression analysis on protein extracts from miRdsRed- and miR669a-injected muscle. (H) Relative quantification for MyHC, MyoD, and Pax7 expression in miRdsRed- and miR669a-treated muscles. P-values are shown (*, $P < 0.01$; **, $P < 0.05$). (I) Morphometric analysis of muscle fibers areas at 7, 14, and 21 d after injury in miRdsRed- and miR669a-injected muscles. It is remarkable that the averaged area of miR669a-treated muscle fibers is extremely reduced (300–500 μm^2) compared with the control muscle fibers (1,000–1,500 μm^2). Four mice per each group of treatment were independently and statistically analyzed using Wilcoxon-Matt-Whitney test ($P < 0.001$). Error bars show means ± SEM. Bars: (A, B, D, and E) 50 µm; (C, C′, F, and F′) 100 µm.

solution containing >4 × 10^5 cpm labeled antisense probe (6× SSC, 5× Denhardt's solution, 1–5 × 10^6 cpm, and 0.2% SDS). After hybridization, the blot was washed in 6× SSC and 0.2% SDS washing solution three times at 50°C. After the final wash, the blot was exposed to x-ray film. miR669q signals were normalized for U2 small nuclear RNA (snRNA; 5′-TTAGCCAAAAGGCCGAGAAGC-3′) hybridization.

miRNAs in situ hybridization

Serial frozen sections from embryos and adult tissues were hybridized overnight at 59°C with biotinylated miR669a/miR669a-like probes previously denatured for 10 min at 70°C in hybridization buffer (200 mM NaCl, 50% formamide, 10% dextran sulfate, 1 mg/ml yeast tRNA, and Denhardt's solution). After 3× 30-min washes in SSC, 50% formamide, and 0.1% Tween, miRNA expression signals were detected using 488 fluorochrome-conjugated streptavidin. Nuclei were stained in blue with DAPI.

Luciferase activity detection

The 3′UTR of MyoD1 and Pax3 mRNA were cloned into the pMIR-REPORT vector (Invitrogen). COS-7 cells were cotransfected with pMIR-REPORT-MyoD1-3′UTR/pMIR-REPORT-Pax3-3′UTR and pre-miR669a (Invitrogen) according to the Lipofectamine 2000 manufacturer's protocol. miRNA scramble precursor was used as a negative control, whereas the pRL-CMV vector was used as an internal control for transfection efficiency. Luciferase activity was detected according to the Dual-Luciferase Reporter Assay System (Promega).

Mutagenesis on MyoD 3′UTR

Mutagenesis experiments were performed according to a site-directed mutagenesis kit (QuickChange II XL; Agilent Technologies). Primers were designed as follows: forward (351CAC353-351TTT353), 5′-GCACAGGGGTGAGCCTTGTTTACCTAAGCCCTGCCCTC-3′, and reverse (351CAC353-351TTT353), 5′-GAGGGCAGGGCTTAGGTAAACAAGGCTCACCCCTGTGC-3′. These primers inserted specific mutations in the 3′UTR of MyoD (mMyoD). The pMIR-REPORT-mMyoD 3′UTR was further amplified by bacterial transformation and selected according to the manufacturer's protocol.

miR669q muscle injections

Adult 4-wk-old male Swiss mice were anesthetized by i.p. injection of a mixture of 5 mg/ml ketamine and 1 mg/ml xylazine. TA muscles were injected with a 100-µl solution containing 10 µM ctx and 10 µg of either miR669q and scramble miRNAs (Invitrogen). 21 d after injection, TA muscles were dissected and immediately frozen in isopentane cooled in liquid nitrogen and stored at −80°C for further analysis.

Microscope image acquisition

Image acquisition was performed with a fluorescent inverted microscope (Eclipse Ti-U; Nikon) equipped with a camera (QICAM Fast 1354; QImaging) using Image-Pro Plus software (Media Cybernetics) and CFI Achromat Series objective lenses (Nikon) detailed as follows: CFI Achromat 10×, NA 0.25; CFI Achromat LWD 20×, NA 0.40; and CFI Achromat 60×, NA 0.80. Transmitted light microscopy images were collected using phase-contrast objectives and rings. When direct comparisons of fluorescence signal levels were needed, wt and knockout treated and untreated cells were processed side by side, and images were collected the same day using constant exposure times. Images were imported in Photoshop (Adobe), assembled in montages, and enhanced for levels, brightness, and contrast simultaneously to preserve the differences in the signal observed in the original data.

Images of differentiating cells were analyzed by time-lapse confocal microscopy using a confocal microscope (BioStation IM-Q; Nikon). Cells were maintained in differentiation condition (DME 2% HS), 5% CO_2, and 95% humidity for 3 d. Frames were taken every 30 min and analyzed according to the NIS-Elements Advanced Research software (Nikon).

Statistical analysis

Results are given as means ± SEM. Statistical significance was tested using one-way analysis of variance and Student's *t* test, moderate *t* statistic, and limma statistic.

Online supplemental material

Fig. S1 shows isolation and characterization of *Sgcb*-null cardiac progenitors. Fig. S2 shows characterization of *Sgcb*-null aorta and ventricle clones. Fig. S3 shows inhibition of myogenic differentiation in *Sgcb*-null cardiac progenitors. Fig. S4 shows miRNA expression profiling in wt and *Sgcb*-null cardiac progenitors. Fig. S5 shows the miRNA expression profile in embryonic/adult tissues and in mouse/human cardiac progenitors. Video 1 shows that *Sgcb*-null cardiac clones aberrantly differentiate into skeletal myotubes. Video 2 shows that miR669a overexpression inhibits skeletal differentiation in *Sgcb*-null cardiac progenitors. Video 3 shows echocardiogram analysis on nude mice transplanted with *Sgcb*-null cardiac progenitors. Online supplemental material is available at http://www.jcb.org/cgi/content/full/jcb.201011099/DC1.

We are grateful to Catherine Verfaillie, Danny Huylebroeck, and Giuseppe Floris for helpful discussions; Alessandra Alteri, Mariana Loperfido, Silvio Conte, Sjoerd Duim, and Laura Perani for skilled technical assistance; and Shea Carter for English editing. We thank K.P. Campbell for providing *Sgcb*-null mice and Paolo Luban for a kind donation.

This work was supported by: the Nash Avery Stem Cell Research–Wicka Fund, University of Minnesota; the Fonds Wetenschappelijk Onderzoek Odysseus Program grant G.0907.08; Research Council of the University of Leuven grant OT/09/053; Cardio Repair European Multidisciplinary Initiative grant 242038 FP7-EC; the Italian Ministry of University and Scientific Research grant 2008RFNT8T_003 (Progetto di Ricerca di Interesse Nazionale 2008); and Cariplo grants 2007.5639 and 2008.2005 to M. Sampaolesi. S. Crippa was supported by Fonds Wetenschappelijk Onderzoek grant ETH-B9008-ASP/08.

Submitted: 18 November 2010
Accepted: 31 May 2011

References

Anversa, P., A. Leri, and J. Kajstura. 2006. Cardiac regeneration. *J. Am. Coll. Cardiol.* 47:1769–1776. doi:10.1016/j.jacc.2006.02.003

Bartel, D.P. 2004. MicroRNAs: genomics, biogenesis, mechanism, and function. *Cell.* 116:281–297. doi:10.1016/S0092-8674(04)00045-5

Beltrami, A.P., K. Urbanek, J. Kajstura, S.M. Yan, N. Finato, R. Bussani, B. Nadal-Ginard, F. Silvestri, A. Leri, C.A. Beltrami, and P. Anversa. 2001. Evidence that human cardiac myocytes divide after myocardial infarction. *N. Engl. J. Med.* 344:1750–1757. doi:10.1056/NEJM200106073442303

Beltrami, A.P., L. Barlucchi, D. Torella, M. Baker, F. Limana, S. Chimenti, H. Kasahara, M. Rota, E. Musso, K. Urbanek, et al. 2003. Adult cardiac stem cells are multipotent and support myocardial regeneration. *Cell.* 114:763–776. doi:10.1016/S0092-8674(03)00687-1

Beltrami, A.P., D. Cesselli, N. Bergamin, P. Marcon, S. Rigo, S. Burelli, E. Puppato, F. D'Aurizio, M. Bottecchia, P. Masolini, et al. 2005. Investigation on possible cell sources to be utilized for cardiac cell therapy. *Pathologica.* 97:185.

Bi, F., N. Liu, and D. Fan. 2003. Small interfering RNA: a new tool for gene therapy. *Curr. Gene Ther.* 3:411–417. doi:10.2174/1566523034578203

Bu, L., X. Jiang, S. Martin-Puig, L. Caron, S. Zhu, Y. Shao, D.J. Roberts, P.L. Huang, I.J. Domian, and K.R. Chien. 2009. Human ISL1 heart progenitors generate diverse multipotent cardiovascular cell lineages. *Nature.* 460:113–117. doi:10.1038/nature08191

Cardinali, B., L. Castellani, P. Fasanaro, A. Basso, S. Alemà, F. Martelli, and G. Falcone. 2009. Microrna-221 and microrna-222 modulate differentiation and maturation of skeletal muscle cells. *PLoS ONE.* 4:e7607. doi:10.1371/journal.pone.0007607

Chen, J.F., E.M. Mandel, J.M. Thomson, Q. Wu, T.E. Callis, S.M. Hammond, F.L. Conlon, and D.Z. Wang. 2005. The role of microRNA-1 and microRNA-133 in skeletal muscle proliferation and differentiation. *Nat. Genet.* 38:228–233. doi:10.1038/ng1725

Crist, C.G., D. Montarras, G. Pallafacchina, D. Rocancourt, A. Cumano, S.J. Conway, and M. Buckingham. 2009. Muscle stem cell behavior is modified by microRNA-27 regulation of Pax3 expression. *Proc. Natl. Acad. Sci. USA.* 106:13383–13387. doi:10.1073/pnas.0900210106

Dellavalle, A., M. Sampaolesi, R. Tonlorenzi, E. Tagliafico, B. Sacchetti, L. Perani, A. Innocenzi, B.G. Galvez, G. Messina, R. Morosetti, et al. 2007. Pericytes of human skeletal muscle are myogenic precursors distinct from satellite cells. *Nat. Cell Biol.* 9:255–267. doi:10.1038/ncb1542

Durbeej, M., R.D. Cohn, R.F. Hrstka, S.A. Moore, V. Allamand, B.L. Davidson, R.A. Williamson, and K.P. Campbell. 2000. Disruption of the beta-sarcoglycan gene reveals pathogenetic complexity of limb-girdle muscular dystrophy type 2E. *Mol. Cell.* 5:141–151. doi:10.1016/S1097-2765(00)80410-4

Galvagni, F., E. Cartocci, and S. Oliviero. 1998. The dystrophin promoter is negatively regulated by YY1 in undifferentiated muscle cells. *J. Biol. Chem.* 273:33708–33713. doi:10.1074/jbc.273.50.33708

Galvez, B.G., M. Sampaolesi, A. Barbuti, A. Crespi, D. Covarello, S. Brunelli, A. Dellavalle, S. Crippa, G. Balconi, I. Cuccovillo, et al. 2008. Cardiac mesoangioblasts are committed, self-renewable progenitors, associated with small vessels of juvenile mouse ventricle. *Cell Death Differ.* 15:1417–1428. doi:10.1038/cdd.2008.75

Galvez, B.G., D. Covarello, R. Tolorenzi, S. Brunelli, A. Dellavalle, S. Crippa, S.A. Mohammed, L. Scialla, I. Cuccovillo, F. Molla, et al. 2009. Human cardiac mesoangioblasts isolated from hypertrophic cardiomyopathies are greatly reduced in proliferation and differentiation potency. *Cardiovasc. Res.* 83:707–716. doi:10.1093/cvr/cvp159

Hotárková, S., M. Hermanová, V. Povýsilová, K. Dvorák, J. Feit, Z. Lukás, L. Kren, P. Vit, H. Jicínská, and B. Hucín. 2004. Demonstration of MyoD1 expression in oncocytic cardiomyopathy: report of two cases and review of the literature. *Pathol. Res. Pract.* 200:59–65. doi:10.1016/j.prp.2004.01.003

Kuzmin, A., Z. Han, M.C. Golding, M.R. Mann, K.E. Latham, and S. Varmuza. 2008. The PcG gene Sfmbt2 is paternally expressed in extraembryonic tissues. *Gene Expr. Patterns*. 8:107–116. doi:10.1016/j.modgep.2007.09.005

Laugwitz, K.L., A. Moretti, J. Lam, P. Gruber, Y. Chen, S. Woodard, L.Z. Lin, C.L. Cai, M.M. Lu, M. Reth, et al. 2005. Postnatal isl1+ cardioblasts enter fully differentiated cardiomyocyte lineages. *Nature*. 433:647–653. doi:10.1038/nature03215

Liang, R., D.J. Bates, and E. Wang. 2009. Epigenetic Control of MicroRNA Expression and Aging. *Curr. Genomics*. 10:184–193. doi:10.2174/138920209788185225

Liu, N., S. Bezprozvannaya, A.H. Williams, X. Qi, J.A. Richardson, R. Bassel-Duby, and E.N. Olson. 2008. microRNA-133a regulates cardiomyocyte proliferation and suppresses smooth muscle gene expression in the heart. *Genes Dev.* 22:3242–3254. doi:10.1101/gad.1738708

McCarthy, J.J. 2008. MicroRNA-206: the skeletal muscle-specific myomiR. *Biochim. Biophys. Acta*. 1779:682–691.

Menasché, P., O. Alfieri, S. Janssens, W. McKenna, H. Reichenspurner, L. Trinquart, J.T. Vilquin, J.P. Marolleau, B. Seymour, J. Larghero, et al. 2008. The Myoblast Autologous Grafting in Ischemic Cardiomyopathy (MAGIC) trial: first randomized placebo-controlled study of myoblast transplantation. *Circulation*. 117:1189–1200. doi:10.1161/CIRCULATIONAHA.107.734103

Nadal-Ginard, B., P. Anversa, J. Kajstura, and A. Leri. 2005. Cardiac stem cells and myocardial regeneration. *Novartis Found. Symp.* 265:142–154. doi:10.1002/0470091452.ch12

Oh, H., S.B. Bradfute, T.D. Gallardo, T. Nakamura, V. Gaussin, Y. Mishina, J. Pocius, L.H. Michael, R.R. Behringer, D.J. Garry, et al. 2003. Cardiac progenitor cells from adult myocardium: homing, differentiation, and fusion after infarction. *Proc. Natl. Acad. Sci. USA*. 100:12313–12318. doi:10.1073/pnas.2132126100

Oh, H., X. Chi, S.B. Bradfute, Y. Mishina, J. Pocius, L.H. Michael, R.R. Behringer, R.J. Schwartz, M.L. Entman, and M.D. Schneider. 2004. Cardiac muscle plasticity in adult and embryo by heart-derived progenitor cells. *Ann. NY Acad. Sci.* 1015:182–189. doi:10.1196/annals.1302.015

Quaini, F., K. Urbanek, A.P. Beltrami, N. Finato, C.A. Beltrami, B. Nadal-Ginard, J. Kajstura, A. Leri, and P. Anversa. 2002. Chimerism of the transplanted heart. *N. Engl. J. Med.* 346:5–15. doi:10.1056/NEJMoa012081

Sampaolesi, M., T. Yoshida, Y. Iwata, H. Hanada, and M. Shigekawa. 2001. Stretch-induced cell damage in sarcoglycan-deficient myotubes. *Pflugers Arch.* 442:161–170. doi:10.1007/s004240100516

Sampaolesi, M., Y. Torrente, A. Innocenzi, R. Tonlorenzi, G. D'Antona, M.A. Pellegrino, R. Barresi, N. Bresolin, M.G. De Angelis, K.P. Campbell, et al. 2003. Cell therapy of alpha-sarcoglycan null dystrophic mice through intra-arterial delivery of mesoangioblasts. *Science*. 301:487–492. doi:10.1126/science.1082254

Sampaolesi, M., S. Blot, G. D'Antona, N. Granger, R. Tonlorenzi, A. Innocenzi, P. Mognol, J.L. Thibaud, B.G. Galvez, I. Barthélémy, et al. 2006. Mesoangioblast stem cells ameliorate muscle function in dystrophic dogs. *Nature*. 444:574–579. doi:10.1038/nature05282

Santerre, R.F., K.R. Bales, M.J. Janney, K. Hannon, L.F. Fisher, C.S. Bailey, J. Morris, R. Ivarie, and C.K. Smith II. 1993. Expression of bovine myf5 induces ectopic skeletal muscle formation in transgenic mice. *Mol. Cell. Biol.* 13:6044–6051.

Shin, C., J.W. Nam, K.K. Farh, H.R. Chiang, A. Shkumatava, and D.P. Bartel. 2010. Expanding the microRNA targeting code: functional sites with centered pairing. *Mol. Cell*. 38:789–802. doi:10.1016/j.molcel.2010.06.005

Tonlorenzi, R., A. Dellavalle, E. Schnapp, G. Cossu, and M. Sampaolesi. 2007. Isolation and characterization of mesoangioblasts from mouse, dog, and human tissues. *Curr. Protoc. Stem Cell Biol.* Chapter 2:2B: 1.

Urbanek, K., D. Torella, F. Sheikh, A. De Angelis, D. Nurzynska, F. Silvestri, C.A. Beltrami, R. Bussani, A.P. Beltrami, F. Quaini, et al. 2005. Myocardial regeneration by activation of multipotent cardiac stem cells in ischemic heart failure. *Proc. Natl. Acad. Sci. USA*. 102:8692–8697. doi:10.1073/pnas.0500169102

van Rooij, E., L.B. Sutherland, X. Qi, J.A. Richardson, J. Hill, and E.N. Olson. 2007. Control of stress-dependent cardiac growth and gene expression by a microRNA. *Science*. 316:575–579. doi:10.1126/science.1139089

van Rooij, E., N. Liu, and E.N. Olson. 2008. MicroRNAs flex their muscles. *Trends Genet.* 24:159–166. doi:10.1016/j.tig.2008.01.007

van Rooij, E., D. Quiat, B.A. Johnson, L.B. Sutherland, X. Qi, J.A. Richardson, R.J. Kelm Jr., and E.N. Olson. 2009. A family of microRNAs encoded by myosin genes governs myosin expression and muscle performance. *Dev. Cell.* 17:662–673. doi:10.1016/j.devcel.2009.10.013

Walowitz, J.L., M.E. Bradley, S. Chen, and T. Lee. 1998. Proteolytic regulation of the zinc finger transcription factor YY1, a repressor of muscle-restricted gene expression. *J. Biol. Chem.* 273:6656–6661. doi:10.1074/jbc.273.12.6656

Williams, A.H., G. Valdez, V. Moresi, X. Qi, J. McAnally, J.L. Elliott, R. Bassel-Duby, J.R. Sanes, and E.N. Olson. 2009. MicroRNA-206 delays ALS progression and promotes regeneration of neuromuscular synapses in mice. *Science*. 326:1549–1554. doi:10.1126/science.1181046

Winitsky, S.O., T.V. Gopal, S. Hassanzadeh, H. Takahashi, D. Gryder, M.A. Rogawski, K. Takeda, Z.X. Yu, Y.H. Xu, and N.D. Epstein. 2005. Adult murine skeletal muscle contains cells that can differentiate into beating cardiomyocytes in vitro. *PLoS Biol.* 3:e87. doi:10.1371/journal.pbio.0030087

Wu, S., R.C. Trievel, and J.C. Rice. 2007. Human SFMBT is a transcriptional repressor protein that selectively binds the N-terminal tail of histone H3. *FEBS Lett.* 581:3289–3296. doi:10.1016/j.febslet.2007.06.025

Yi, B.A., O. Wernet, and K.R. Chien. 2010. Pregenerative medicine: developmental paradigms in the biology of cardiovascular regeneration. *J. Clin. Invest.* 120:20–28. doi:10.1172/JCI40820

Yuasa, K., Y. Hagiwara, M. Ando, A. Nakamura, S. Takeda, and T. Hijikata. 2008. MicroRNA-206 is highly expressed in newly formed muscle fibers: implications regarding potential for muscle regeneration and maturation in muscular dystrophy. *Cell Struct. Funct.* 33:163–169. doi:10.1247/csf.08022

Zuker, M., and A.B. Jacobson. 1998. Using reliability information to annotate RNA secondary structures. *RNA*. 4:669–679. doi:10.1017/S1355838298980116

Published June 27, 2011

Crippa et al., http://www.jcb.org/cgi/content/full/jcb.201011099/DC1

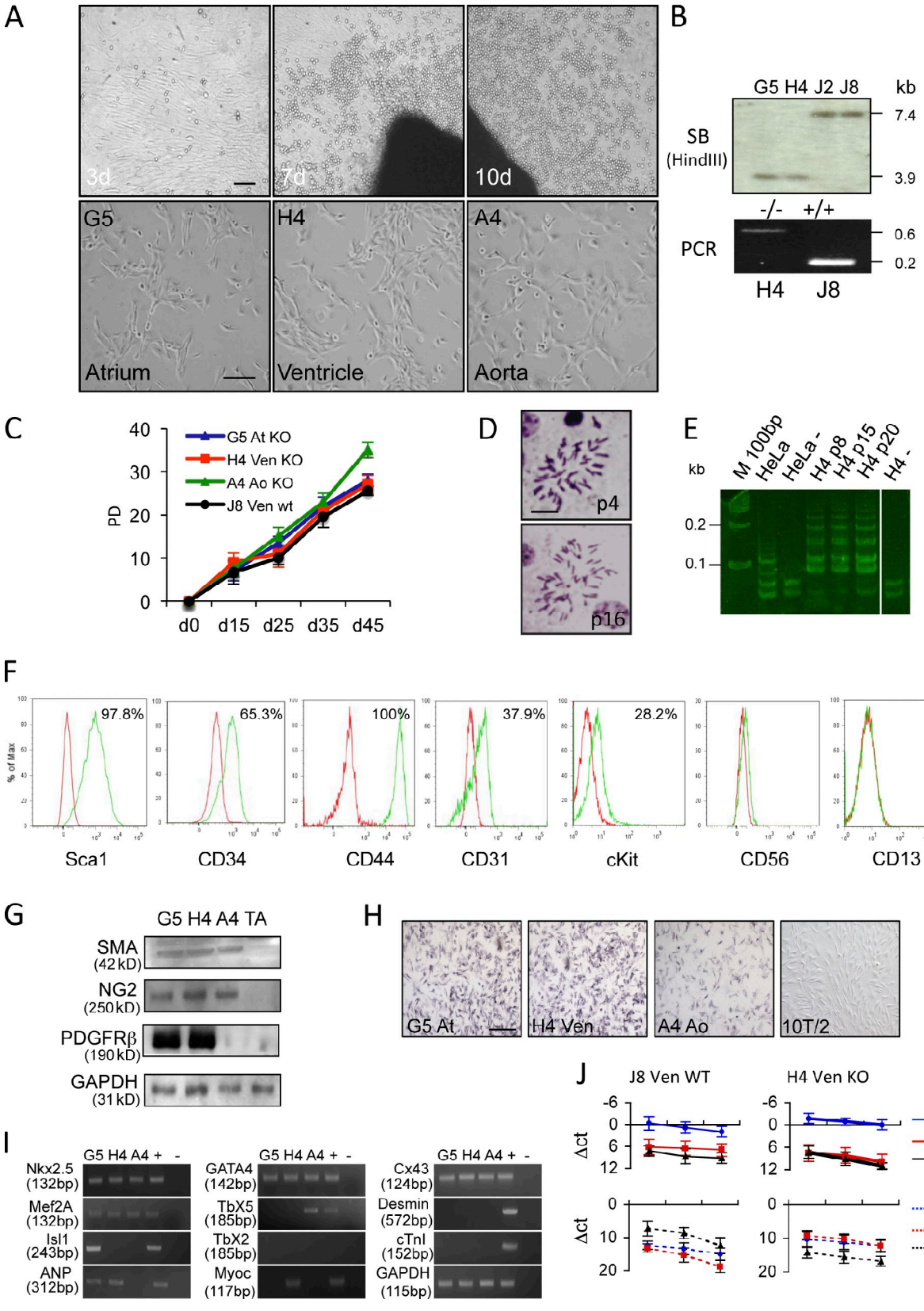

Published June 27, 2011

Figure S1. **Isolation and characterization of *Sgcb*-null cardiac progenitors.** (A) Phase-contrast morphology of cells isolated from fragments of atrium, ventricle, or aorta of adult mice hearts after culturing for 3, 7, and 10 d (top). The rounded and refractile cells are visible on the top of fibroblasts layer at day 7 and 10. Selected confluent clones at early passage from atrium (G5), ventricle (H4), and aorta (A4) derived from dystrophic hearts are shown on the bottom. (B) Southern blot analysis (top) on *Sgcb*-null (G5 and H4) and wt (J2 and J8) clones. DNA was digested with the restriction enzyme HindIII and probed by Southern blotting with a probe against exon 2 of the *Sgcb* gene (see Materials and methods). The replacement of exons 3–6 by the neomycin cassette yields a 3.9-kb HindIII fragment in the *Sgcb*-null genotype and a 7.4-kb HindIII fragment in the wt genotype. An example of genotyping PCR on *Sgcb*-null (H4) and wt (J8) clones is reported in the bottom; primers amplified a 600-bp fragment in the *Sgcb*-null and a 200-bp fragment in the wt. Band sizes are reported. (C) Proliferation curves for three different *Sgcb*-null clones compared with the wt clone (black line). At the time of explant isolation, cell populations were considered to be at one population doubling (PD). (D) Example of karyotype analysis on *Sgcb*-null cardiac progenitors (H4) at p4 and p16. (E) Examples of telomerase activity in *Sgcb*-null ventricle clone (H4) at 8, 15, and 20 population doublings. HeLa cells were used as positive controls; temperature denatured samples were used as negative controls (−). M, marker. (F) *Sgcb*-null clones were analyzed for the expression of Sca-1, CD34, CD44, CD31, c-Kit, neural cell adhesion molecule (NCAM or CD56), and CD13. The percentage of FACS-positive cells is reported at the top of each graph. (G) Western blot analysis for the expression of pericyte markers in *Sgcb*-null clones (G5, H4, and A4). Protein extract from tibialis anterior muscle (TA) was used as a negative control. Smooth muscle actin (SMA), neural–glial-2 chondroitin sulfate proteoglycan (NG2), and platelet-derived growth factor receptor β (PDGFR-β) were measured. Glyceraldehyde 3-phosphate dehydrogenase (GAPDH) was used for sample normalization. Band sizes are reported. (H) AP staining in *Sgcb*-null cardiac progenitors from atrium (G5 atrium [At]), ventricle (H4 Ven), and aorta (A4 aorta [Ao]) at p5. A 10T/2 fibroblast cell line was used as a negative control. (I) RT-PCR for the expression of early (NkX2.5, Mef2A, Isl1, atrial natriuretic peptide, GATA4, Tbx5, Tbx2, and myocardin) and late (Cx43, Desmin, and cTnI) cardiac markers in *Sgcb*-null clones (G5, H4, and A4). Embryo E11 and adult liver cDNA were used as a positive control (+) and a negative control (−), respectively. (J) Time course qPCR for the expression of pericyte markers, SMA, PDGFR-β, and NG2 in wt (J8 Ven WT) and *Sgcb*-null (H4 Ven KO) cardiac progenitors after serum starvation (top). Time course qPCR analysis for the expression of cardiac markers Nkx2.5, GATA4, and Mef2A in wt (J8 Ven WT) and *Sgcb*-null (H4 Ven KO) progenitors after serum starvation (bottom). Ct, cycle threshold. All experiments were performed in triplicates and statistically analyzed. Error bars show means ± SEM. Bars: (A and H) 50 µm; (D) 10 µm.

Published June 27, 2011

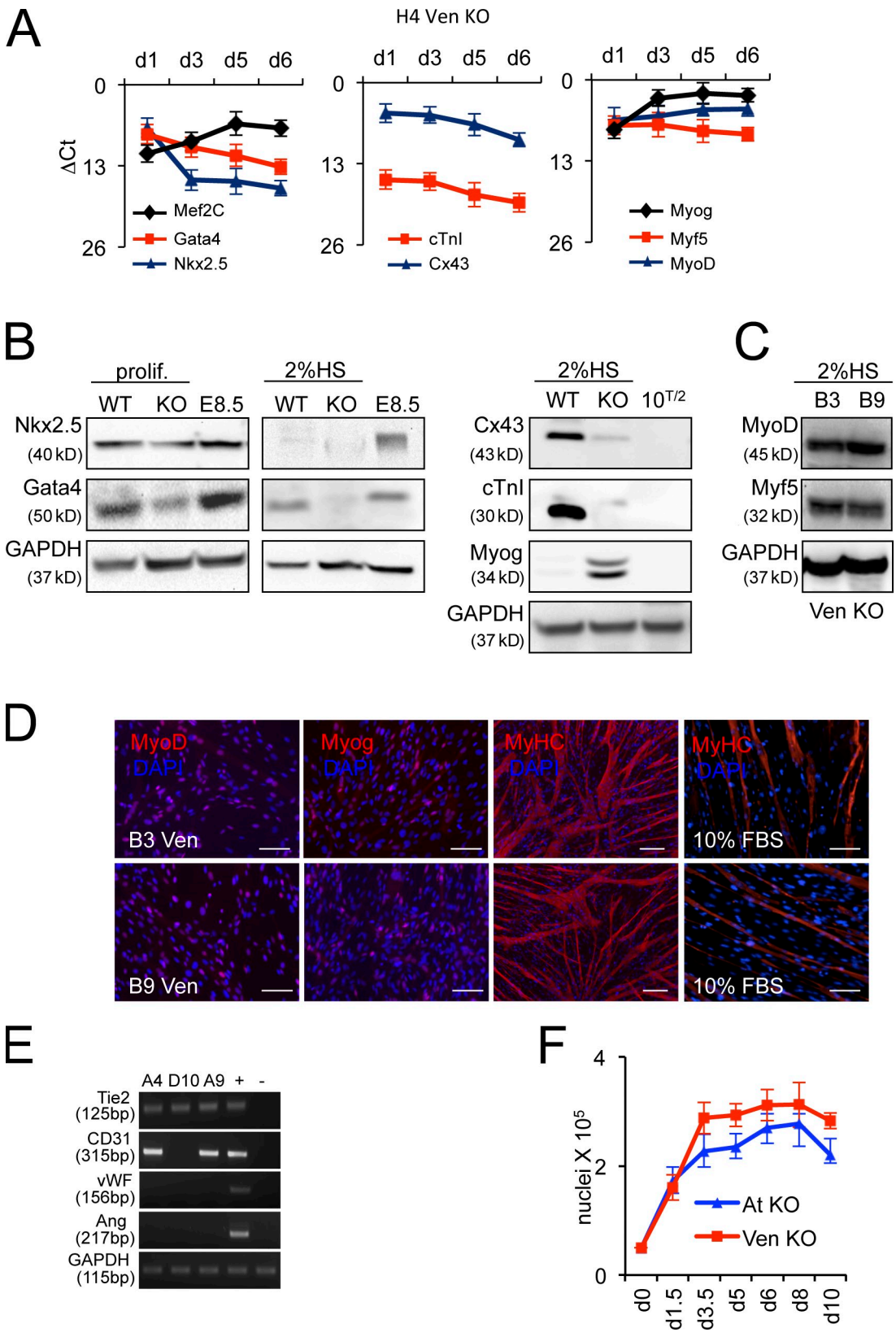

Figure S2. **Characterization of *Sgcb*-null aorta and ventricle clones.** (A) Time course (day 1, 3, 5, and 6) analysis for the expression of early cardiac (Mef2C, GATA4, and Nkx2.5), late cardiac (cTnI and Cx43), and muscle (Myog, Myf5, and MyoD) genes in differentiating *Sgcb*-null cardiac clones (H4 Ven KO). During differentiation, *Scgb*-null cardiac progenitors repressed the expression of early cardiac markers and up-regulated skeletal muscle transcription factors. Three independent experiments were performed and statistically analyzed. Ct, cycle threshold. (B) Western blot analysis for the expression of early cardiac markers (Nkx2.5 and Gata4) in proliferating (prolif.) and differentiating (2% HS) wild-type (WT) and *Sgcb*-null (KO) cardiac progenitors (left). The protein extract from embryo 8.5 dpc (E8.5) was used as a positive control. Western blot analysis for late cardiac (Cx43 and cTnI) and myogenic

Published June 27, 2011

(Myog) markers expression in differentiated wt and *Sgcb*-null cardiac progenitors (right). Protein extract from 10T/2 fibroblasts was used as negative control. GAPDH was used for sample normalization. (C) Western blot analysis for MyoD and Myf5 expression in two different *Sgcb*-null ventricle clones (B3 and B9) 1 d after serum starvation (2% HS). Proliferating B3 and B9 clones were negative for MyoD expression as shown in Fig. 2 A and, when induced to differentiate, they early up-regulated muscle transcription factors. GAPDH was used for sample normalization. (D) Immunofluorescence analysis on differentiating *Sgcb*-null ventricle clones (top, B3 ventricle; bottom, B9 ventricle). Nuclei were stained in blue with DAPI. Sgcb-null cardiac progenitors differentiate into skeletal myotubes, even in growth medium (DME 10% FBS) at high confluence (85%) as shown by immunofluorescence analysis on proliferating (DME 10% FBS) ventricle clones. (E) PCR analysis for the expression of early (Tie2 and CD31) and late (von Willebrand factor [vWF] and angiopoietin [Ang]) endothelial markers in proliferating *Sgcb*-null aorta clones (A4, A9, and D10). Embryo E11 and adult liver cDNA were used as a positive (+) and a negative control (–), respectively. GAPDH was used for normalization. All clones are positive for Tie2 but negative for late endothelial markers. (F) Proliferation curves for two different *Sgcb*-null cardiac clones (atrium [At] KO and ventricle KO) during 10 d of serum starvation. Cells were counted in triplicates using NucleoCounter. Error bars show means ± SEM. Bars, 50 µm.

Published June 27, 2011

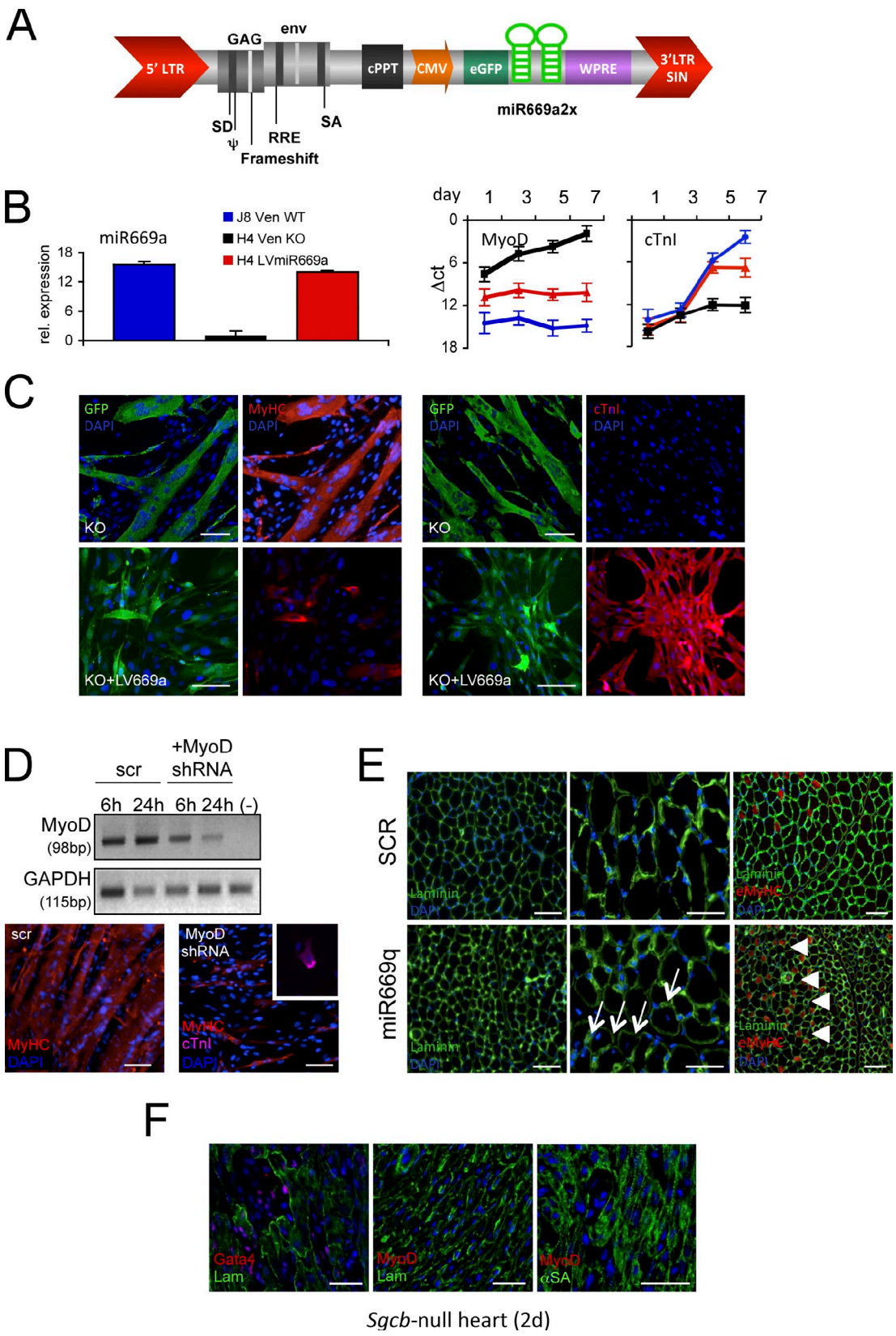

Figure S3. **Inhibition of myogenic potential in *Sgcb*-null cardiac progenitors.** (A) Schematic representation of pLentiCMV-EGFP-miR669a2× was used to overexpress miR669a in *Sgcb*-null clones. SA, splice acceptor site; SD, splicing donor site; LTR, long terminal repeat; GAG, glycosaminoglycan; env, envelope; cPPT, central polypurine tract; CMV, cytomegalovirus; RRE, Rev response element; SIN, self inactivating; WPRE, woodchuck hepatitis virus posttranscriptional regulatory element. (B) TaqMan assay analysis for the expression of miR669a in a H4 *Sgcb*-null clone transduced with pLentiCMV-EGFP-miR669a2× compared with wt and Sgcb-null clones (left). Time course analysis (day 1, 3, 5, and 7) for MyoD and cTnI expression in J8 Ven wt (blue line), H4 Ven KO (black line), and H4 LVmiR669a (red line). Note that differentiation toward cardiac lineage was partially rescued in H4 LVmiR669a that reduced MyoD ex-

Published June 27, 2011

pression and up-regulated cTnI after 3 d of serum starvation. rel., relative. (C) Immunofluorescence analysis for GFP and MyHC expression in H4 ventricle KO (top left) and H4 LVmiR669a (bottom left). Skeletal myogenesis was inhibited in miR669a transduced *Sgcb*-null progenitors. Immunofluorescence analysis for GFP and cTnI in H4 Ven KO (top right) and H4 LVmiR669a (bottom right) cardiac clones. Cardiac myogenesis was activated in the miR669a transduced clone. (D) PCR analysis for MyoD expression in *Sgcb*-null cardiac progenitors 6 and 24 h after transfection with scrambled (scr) and MyoD shRNA. 10T/2 fibroblast cDNA was used as negative control (–). GAPDH expression was analyzed for sample normalization (top). Immunofluorescence analysis on *Sgcb*-null cardiac progenitors transfected with scrambled (bottom) and MyoD shRNA (bottom right). A cTnI-positive cell is shown at a high magnification in the inset. (E) Immunofluorescence analysis of TA muscle sections 21 d after injection with 10 µm ctx and 10 µg of either scramble miRNAs (SCR) or mir669q ($n = 3$ per each group of treatment). Embryonic MyHC (eMyHC) was stained in red on the right. The higher number of center nucleated fibers (arrows), which are smaller in diameter and positive for embryonic MyHC (highlighted by arrowheads), in miR669q-injected muscles indicated a delay in the regenerative process. (F) Example of immunofluorescence analysis on cardiac sections from 2-d-old *Sgcb*-null mice ($n = 3$). Neonatal hearts are positive for Gata4 expression (left) but negative for the expression of MyoD (middle and right). Double staining of *Sgcb*-null cardiac sections with MyoD and α sarcomeric actin (αSA) is reported on the right. Nuclei are stained in blue with DAPI. Error bars show means ± SEM. Bars, 50 µm.

Published June 27, 2011

A

probeID	Sgcb-null/wt	probeID	Sgcb-null/wt
mmu-miR-206_st	7,737378955	mmu-miR-146b_st	-3,774857303
mmu-miR-486_st	3,100099817	mmu-miR-467a_st	-3,437000938
mmu-miR-699_st	3,233267238	mmu-miR-652_st	-2,716961783
mmu-miR-149_st	2,645310472	mmu-miR-181a_st	-2,063688447
mmu-miR-196a_st	3,180733289	mmu-miR-152_st	-2,578045927
mmu-miR-18a_st	2,061621679	mmu-miR-297a_st	-3,208692432
mmu-miR-421_st	2,871439461	mmu-miR-199b-star_st	-2,40856526
mmu-miR-130b_st	2,801361465	mmu-miR-455_st	-2,969599051
mmu-miR-378-star_st	2,351821564	mmu-miR-16-star_st	-2,281241468
mmu-miR-615-3p_st	2,388298317	mmu-miR-466j_st	-2,863527824
mmu-miR-1198_st	1,680053593	mmu-miR-466f_st	-2,262598776
mmu-miR-532-5p_st	1,41712022	mmu-miR-466h_st	-2,636926727
mmu-miR-92a_st	1,743210112	mmu-miR-99a_st	-1,906962272
mmu-miR-21-star_st	1,809281453	mmu-miR-130a_st	-1,266324544
mmu-miR-27b-star_st	1,920112498	mmu-miR-466f-5p_st	-2,043765611
mmu-miR-106a_st	1,215987486	mmu-miR-669c_st	-2,548271314
mmu-miR-335-5p_st	1,659851156	mmu-miR-574-3p_st	-1,701678302
mmu-miR-20a_st	1,434838701	mmu-miR-346_st	-1,701141074
mmu-miR-27a-star_st	1,623937435	mmu-miR-669a_st	-1,774320688
mmu-miR-712_st	2,853457511	mmu-miR-674_st	-1,201852432
mmu-miR-17_st	1,163046089	mmu-miR-1187_st	-1,707528907
mmu-miR-362-5p_st	1,351226854	mmu-miR-199a-3p_st	-1,145796724
mmu-miR-1192_st	1,303458822	mmu-miR-466b-3p_st	-1,43919163
mmu-miR-532-3p_st	1,939433935	mmu-miR-125b-5p_st	-1,1577115
mmu-miR-133b_st	2,9631416	mmu-miR-26a_st	-1,354257516
mmu-miR-714_st	1,779052233	mmu-miR-1196_st	-1,273796216
mmu-miR-715_st	1,232363094	mmu-miR-669b_st	-2,037289783
mmu-miR-145_st	1,034272909	mmu-miR-34c_st	-1,282816145
		mmu-miR-466e-3p_st	-1,011619062
		mmu-miR-140-star_st	-1,102681403
		mmu-miR-342-3p_st	-1,032364522
		mmu-miR-199b_st	-1,116458962

B

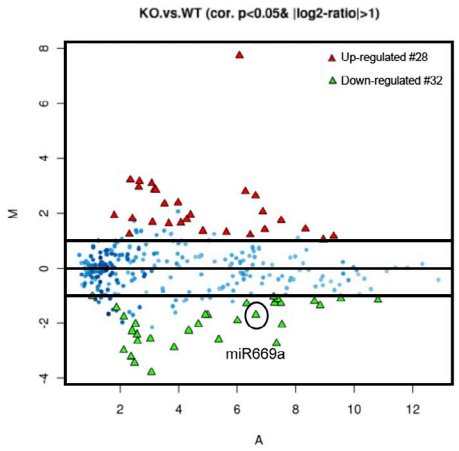

C

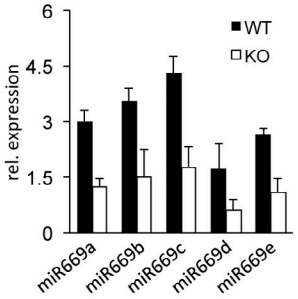

D

```
UACAUGUGUGUGCAUGUGUGUA   miR669q

 AGUUGUGUGUGCAUGUUCAUGU  miR669a
 AGUUUUGUGUGCAUGUGCAUGU  miR669b
AUAGUUGUGUGUGGAUGUGUGU   miR669c
 ACUUGUGUGUGCAUGUAUAUGU  miR669d
UGUCUUGUGUGUGCAUGUUCAU   miR669e
```

E

```
3' tgtacttGtACGTGTGtgTTgat 5' miR669a
        | |||||||  ||
5' gtgagcCtTGCACACctAAgcc 3' MyoD 3'UTR

3' tAgTgtGtACGTGTGtgTaCat 5' miR669q
     | |  | |||||||  | |
5' gTgAgcCtTGCACACctAaGcc 3' MyoD 3'UTR
```

F

```
3' tgtacttGtACGTGTGtgTTgat 5' miR669a
        | ||   ||  ||
5' gTgAgcCtTGTTTACctAaGcc 3' MyoD 3'UTR
        | ||   ||  | |
3' tAgTgtGtACGTGTGtgTaCat 5' miR669q
```

G

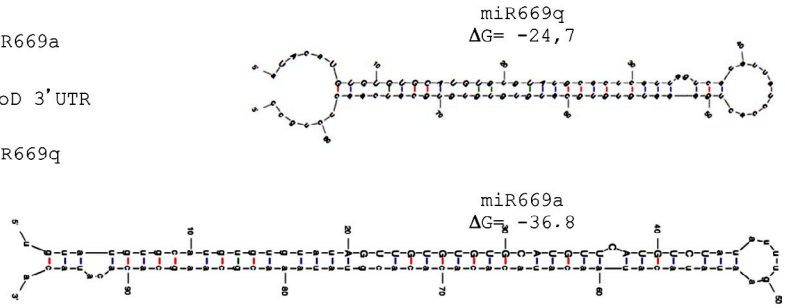

Figure S4. **miRNA expression profiling in wt and *Sgcb*-null cardiac progenitors.** (A) List of miRNAs differently regulated in *Sgcb*-null versus wt cardiac progenitors. Among the miRNAs analyzed in the GeneChip, 28 and 32 miRNAs were up-regulated and down-regulated, respectively, in *Sgcb*-null clones compared with the wt counterparts. Probe IDs indicate the miRNAs spotted and analyzed in the Affymetrix commercial platform used for miRNA array analysis. (B) MA plot representing the average intensities versus the $\log_2$ ratios. The $\log_2$ ratios in the MA plot are based on the limma estimates. The dots are colored in green and in red if they are classified as down- and up-regulated, respectively, based on the Benjamini-Hochberg–corrected p-values (right) and an absolute $\log_2$ fold change >1. miR669a's rank is highlighted by a black circle. Blue dots in indicate those miRNA that are similarly expressed in wt and *Sgcb*-null

Published June 27, 2011

cardiac progenitors. (C) TaqMan analysis showed that the members of miR669 family with the highest homology to miR669a (miR669b, miR669c, miR669d, and miR669e) are also strongly down-regulated in *Sgcb*-null compared with wt cardiac progenitors. Three independent experiments were performed and statistically analyzed. rel., relative. (D) Schematic representation of sequence homology between miR669q, located in intron 1 of the *Sgcb* gene, miR669a, and the other members of miR669 located in intron 10 of the *Sfmbt2* gene. (E) Schematic representation of miR669a (top) and miR669q (bottom) centered site pairing within the 3′UTR of MyoD. (F) Schematic representation of mutagenesis experiments on MyoD 3′UTR. Mutated nucleotides are highlighted in blue. Red letters indicate the nucleotide mutated within the MyoD 3′UTR. (G) Predicted hairpin structure for mmu-miR-669q ($\Delta G = -24.70$; top). mmu-miR-669a-1 structure is shown in the bottom for comparison ($\Delta G = -36.8$). Of note, the miR669q hairpin resembles a typical hairpin structure, which differs from the other members of miR669 cluster in the position of the mature part. The predicted mature part of miR669q starts at position −36 from the loop, whereas miR669a-1 mature sequence starts at position −25 (conserved positions between 669a and 669q are in capital letters). Red, three hydrogen bonds; blue, two hydrogen bonds; green, mismatch.

Published June 27, 2011

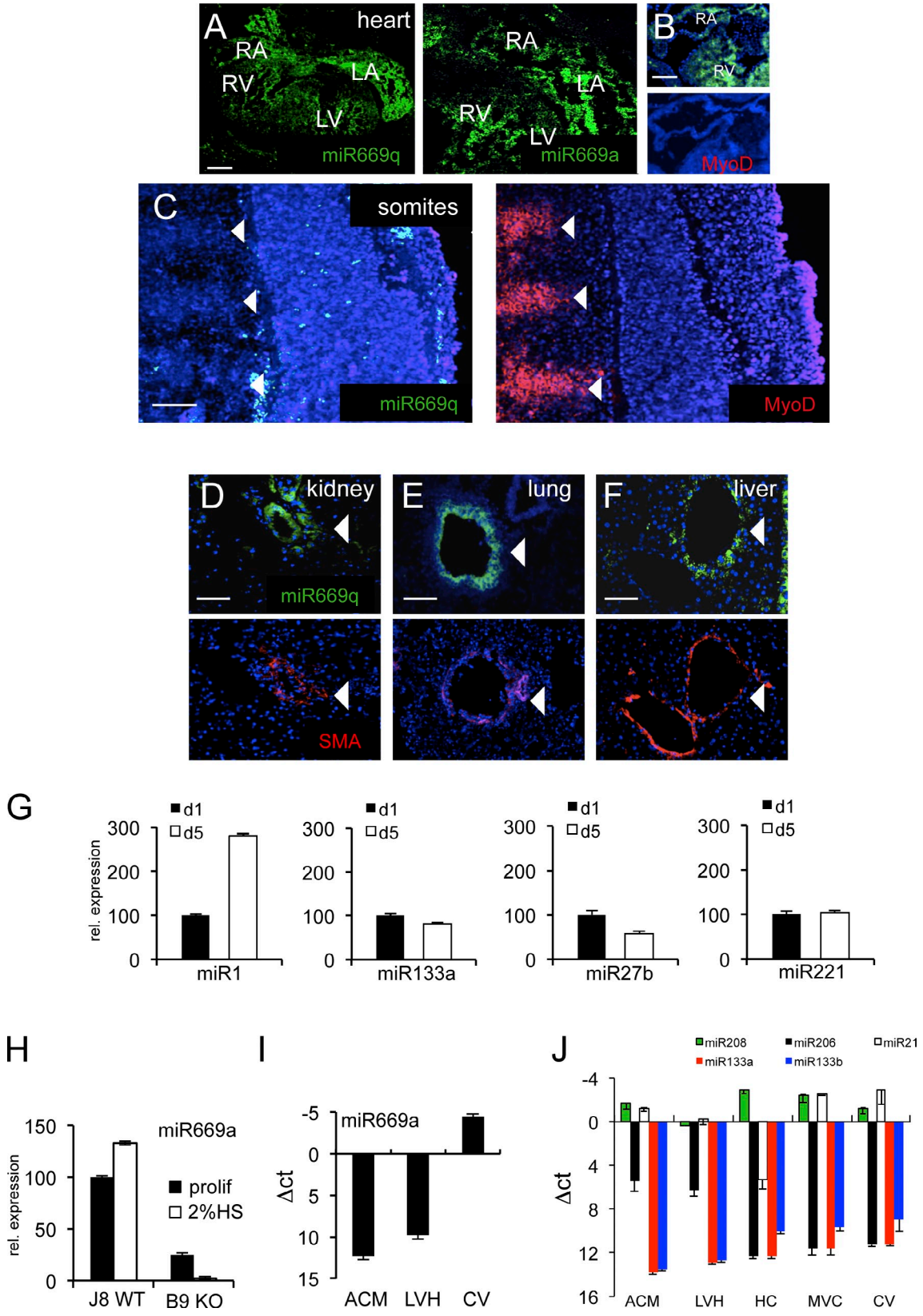

Figure S5. **miRNA expression profile in embryonic/adult tissues and in mouse/human cardiac progenitors.** (A–C) miR669q and miR669a in situ hybridization and MyoD immunostaining on serial sections of different embryonic tissues. (A) miR669q and miR669a in situ hybridization on heart sections from wt embryos at 13.5 dpc. RA, right atrium; LA, left atrium; RV, right ventricle; LV, left ventricle. (B) miR669q in situ hybridization and MyoD immunostaining on serial sections from wt hearts at 11.5 dpc. (C) miR669q in situ hybridization and MyoD immunostaining on sections from wt embryos at 11.5 dpc. miR669q was not expressed in MyoD-positive somites as indicated by the arrowheads. (D–F) miR669q in situ hybridization and SMA immunostaining on serial sections from different adult tissues, i.e., kidney (D), lung (E), and liver (F). (G) TaqMan analysis for the expression of muscle-related miRNAs (miR1,

Published June 27, 2011

miR133a, miR27b, and miR221) in differentiating *Sgcb*-null cardiac progenitors at 1 and 5 d after serum starvation. (H) TaqMan assay analysis for miR669a expression in *Sgcb*-null ventricle clone (B9). miR669a was strongly down-regulated during differentiation in correlation with MyoD expression. (I) TaqMan assay analysis for the expression of miR669a in cardiac progenitors isolated from patients affected by different forms of cardiac disease (ACM, acute myocardial infarction; LVH, left ventricular hypertrophy; CV, cardiac valvulopathy). (J) TaqMan assay analysis for the expression of cardiac and skeletal muscle-related miRNAs in human cardiac progenitors isolated from patients affected by different forms of chronic cardiac disease (HC, hypertrophic cardiomyopathy; MVC, mitral valvular cardiomyopathy). It is noteworthy that all human cardiac clones highly expressed miR208, which was shown to be involved in cardiac hypertrophy, fibrosis, and expression of β-MHC in response to cardiac stress. miR206 was overexpressed in acute myocardial infarction and left ventricular hypertrophy clones; miR21 was less enriched in the hyperthropic cardiomyopathy clone; miR133a was equally and poorly expressed by all the clones, whereas miR133b was lightly overexpressed in mitral valvular cardiomyopathy, and cardiac valvulopathy clones. Three independent experiments were performed and statistically analyzed for all panels. rel., relative. Error bars represent means ± SEM. Bars, 50 µm.

Published June 27, 2011

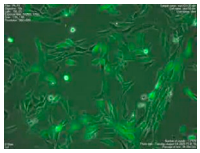

Video 1. ***Sgcb*-null cardiac clones aberrantly differentiate into skeletal myotubes.** An H4 *Sgcb*-null clone transduced with the reporter gene GFP (LV-CMV-GFP) was induced to differentiate by serum starvation. Images were analyzed by time-lapse confocal microscopy (BioStation IM-Q). Frames were taken every 30 min for 3 d (30 min/6 frames per second).

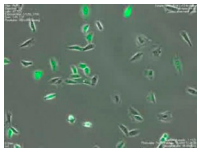

Video 2. **miR669a overexpression inhibits skeletal muscle differentiation in *Sgcb*-null cardiac progenitors.** An H4 *Sgcb*-null clone transduced with a lentiviral vector overexpressing GFP and two copies of pre-miR669a under the control of the CMV promoter was induced to differentiate by serum starvation. Images were analyzed by time-lapse confocal microscopy (BioStation IM-Q). Frames were taken every 30 min for 3 d (30 min/6 frames per second).

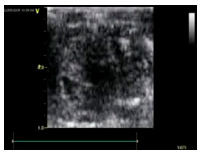

Video 3. **Example of echocardiogram analysis on nude mice transplanted with *Sgcb*-null cardiac progenitors.** Cardiac functionality of nude mice transplanted with 5×10^5 GFP transduced H4 *Sgcb*-null clone was analyzed 8 wk after cell transplantation by Vevo 2100 (Visual Sonics).